TYPE Original Research
PUBLISHED 04 October 2024
DOI 10.3389/fmars.2024.1457964

Mineralogy and geochemistry of the Cambrain Shuijingtuo Formation black shales from Western Hubei, China: implications on enrichment of critical metals and paleoenvironment

Yuan Wang[1], Jing Li[1*], Yang Lin[1], Xinguo Zhuang[1], Vanlong Hoang[2], Peng Wu[1], Xin Luo[1], Han Zhang[1] and Xiaoyang Zhang[1]

[1]Key Laboratory of Tectonics and Petroleum Resources of Ministry of Education, China University of Geosciences, Wuhan, China, [2]Exploration & Production Center, Vietnam Petroleum Institute, Hanoi, Vietnam

Check for updates

OPEN ACCESS

EDITED BY
Xiaodong Jiang,
Guangdong University of Technology, China

REVIEWED BY
Rui Bao,
Ocean University of China, China
Mabrouk Sami,
United Arab Emirates University,
United Arab Emirates

*CORRESPONDENCE
Jing Li
jingli@cug.edu.cn

RECEIVED 01 July 2024
ACCEPTED 13 September 2024
PUBLISHED 04 October 2024

CITATION
Wang Y, Li J, Lin Y, Zhuang X, Hoang V, Wu P, Luo X, Zhang H and Zhang X (2024) Mineralogy and geochemistry of the Cambrain Shuijingtuo Formation black shales from Western Hubei, China: implications on enrichment of critical metals and paleoenvironment. *Front. Mar. Sci.* 11:1457964. doi: 10.3389/fmars.2024.1457964

Black shales have attracted the attention of numerous researchers not only due to their high potential as hydrocarbon source rocks and shale gas reservoirs, but also to the enrichment of critical metal elements in black shale series. Black shale of the Cambrian Shuijingtuo Formation is one of the most important black shales in the Yangtze platform. This paper conducts integrated research on the mineralogical and geochemical characteristics of this black shale from the Luojiacun section in Western Hubei Region, aiming at elaborating the enrichment mechanism of elevated critical metal elements in the Shuijingtuo black shale. Minerals in the Shuijingtuo black shale are predominantly composed of quartz (avg. 43.0%) and clay minerals (avg. 32.5%), with small proportions of calcite, albite, clinochlore, and pyrite. The Shuijingtuo black shale is characterized by high total organic carbon (TOC, avg. 3.9%) content and enriched in V-Ni-Cr-U and Sr-Ba critical metal assemblages. The elevated V, Cr, Ni, and U present dominant organic affinities, while Sr and Ba are closely correlated to calcite and pyrite, respectively. The enrichment of V-Cr-Ni-U critical element assemblages in Shuijingtuo black shale are ascribed to the high primary productivity, anoxic depositional conditions, marine biologic production, and low-temperature hydrothermal activities. The enrichment of Sr and Ba is related to the high primary productivity and anoxic depositional conditions, respectively.

KEYWORDS
critical elements, enrichment mechanism, palaeoredox environment, organic-rich black shale, Shuijingtuo Formation, Western Hubei region

1 Introduction

Black shales are commonly considered as potential hydrocarbon source rocks and shale gas reservoirs because of the high total organic carbon (TOC) content (Gao et al., 2019; Yan et al., 2021), which contribute to large proportions of Proterozoic and Palaeozoic hydrocarbons and play important roles in oil and gas development worldwide (Luning et al., 2000; Wu et al., 2015). Moreover, a variety of important elements, including V, Mn, Ni, Mo, U, Ba, and P are significantly enriched with high grade and large scale in these black shale series in some areas (Ye and Fan, 2000; Fathy et al., 2024), which have a promising economic potential. Consequently, research on black shales is of important economic significance for both hydrocarbon and polymetallic extraction. Furthermore, due to the occurrence of several particular geological events (e.g., mass extinctions, biodiversity change, oceanic anoxia, and continental glaciation) during the deposition process of black shales (Armstrong et al., 2009; Delabroye and Vecoli, 2010; Yan et al., 2010; Sheets et al., 2016; Trela et al., 2016; Pohl et al., 2017), research on black shales is of important theoretical significance as well, which can correspondingly provide valuable information for these geological events (Ghosh and Sarkar, 2010; Dai et al., 2018; Yan et al., 2021).

Black shale of the Niutitang Formation (corresponding to the Shuijingtuo Formation in this paper) is a set of shale with great gas potential in South China. A large number of scholars have carried out studies on the evaluation of pore characteristics and gas potential, sources of organic matter, geochemical characteristics of rare earth elements and restoration of sedimentary environment in the Niutitang Formation black shale (Yin et al., 2017; Wan et al., 2018; Xi et al., 2018; Tian et al., 2019; Liu et al., 2020; Wu et al., 2020; Zhang et al., 2021; Awan et al., 2022; Li et al., 2022; Wei et al., 2022). In particular, research on mineralogical and geochemical characteristics of the Shuijingtuo black shale composition is of crucial significance because they have been widely used as important indicators for ancient seawater chemistry, palaeomarine environment conditions, and source compositions of detrital sediments (Algeo and Maynard, 2004; Algeo and Rowe, 2012; Dai et al., 2013b) due to their predictable behavior during different geological processes (Ghosh and Sarkar, 2010; Dai et al., 2014, 2017).

However, due to the heterogeneity in chemical composition of black shales, the mineralogical and geochemical characterization of these shales remains contentious, let alone the enrichment mechanism of strategic metal elements in black shales (Han et al., 2018). In the current study, the mineralogical and geochemical characteristics of black shales of the Cambrian Shuijingtuo Formation from Western Hubei Region are elaborated, with emphasis on the abundance, occurrence and genesis of potential elevated strategic metals in black shales. This research will provide not only essential mineralogical and geochemical evidences for the provenance composition and depositional paleoenvironment of black shales, but also an objective evaluation on the enrichment of potential strategic metal element resources in black shales.

2 Geological setting

A set of black mudstones and black siliceous rocks with extremely high organic matter content were widely developed and well preserved in the Yangtze platform in the Early Cambrian. The Yangtze platform generally transited from a shallow water platform area to a slope and deep-water basin during the Early Cambrian. Consequently, during this period, the Yangtze platform was roughly divided into four sedimentary facies areas from NW to SE, viz., the inland shelf shallow water platform, the outer shelf depression, the shelf edge upper slope area, and the deep-water basin area (Och et al., 2013; Cremonese et al., 2014; Fu et al., 2016; Zhang et al., 2016).

The western Hubei Region is geotectonically located on the southeast slope of Huangling Uplift in the northwest of the middle of the Yangtze Platform, known as the Yichang slope belt, where the black shales of the Early Cambrian Shuijingtuo Formation are widely distributed (Figure 1A). In the Yichang slope belt, there is a double-layer basement composed of the Kongling complex in the Paleoproterozoic and the intruding Neo-Proterozoic Huangling granite and Xiaofeng basic-ultrabasic rocks, which is held by the western Hubei fold.

The black shales of the Early Cambrian Shuijingtuo Formation were the primary hydrocarbon source rocks and shale gas reservoirs in the studied area, which were mainly deposited in a transitional sedimentary environment from shallow water platform area to the shelf edge upper slope and deep-water basin facies area of the Yangtze platform (Zhu et al., 2015). The Shuijingtuo Formation was lithologically composed of black shales, and unconformably overlay the black mudstones of the Lower Cambrian Yanjiahe Formation (Figure 1B).

3 Sampling and analytical methods

The black shale samples in this study were collected from the lowest part of the Shuijingtuo Formation of the Luojiacun section, which is geographically situated in Zigui county, Yichang city in the Western Hubei Region (Figure 1A). Twenty-six bulk black shale samples were taken with a sampling interval ranging from tens of centimeters to 2 meters (Figure 1B). Each sample was ground to 200 mesh with an agate mortar for mineralogical and geochemical analysis.

The mineral composition of black shale samples was determined by X-ray diffraction analysis (XRD, Bruker D8 A25 Advance), which was carried out on powder diffractometer with monochromatic Cu, Kα radiation. The quantitative content of minerals was subsequently analyzed based on the X-ray diffractograms using Software Jade 6.5.

The morphological characteristics of typical minerals and occurrence of some trace elements in black shales were observed by field emission scanning electron microscope (FE-SEM, FEI Quanta 450 FEG) in conjunction with an energy dispersive X-ray spectrometer (SEM-EDS), which can realize the integrated analysis function of image, composition and structure. SEM images of typical minerals were captured by a retractable solid-state backscatter electron detector.

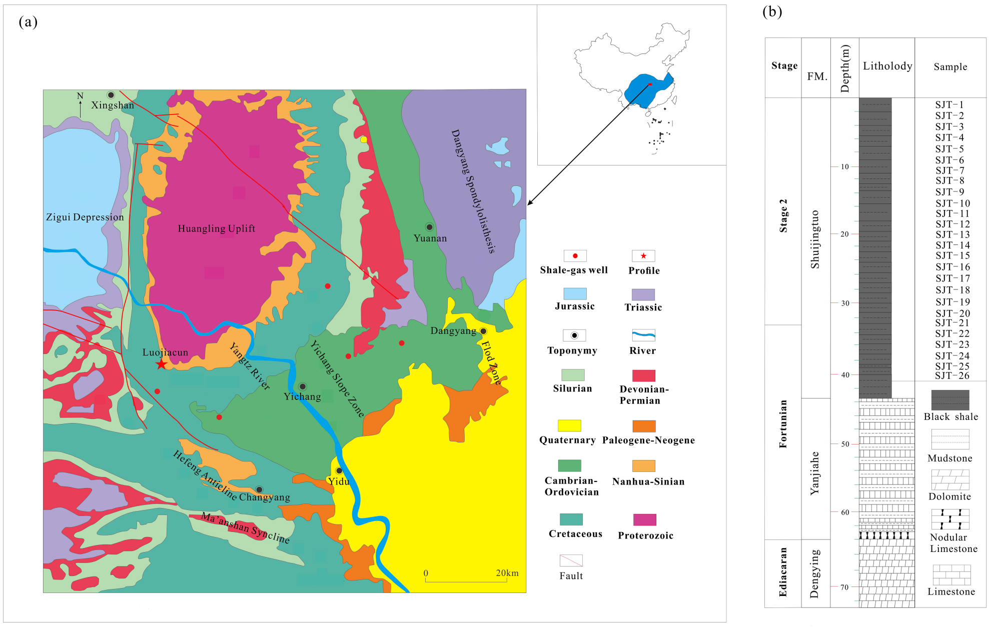

FIGURE 1
(A) Regional geological map of the study area (modified from Chen, 2018); **(B)** sampling column of the Shuingtuo Formation.

The TOC content of black shale samples was determined by a Vario EL III element analyzer with the standard deviation of measurements below ±0.10%. Prior to determination, the black shale samples were first treated by 4 M HCl at 60°C for at least 24 h to remove the carbonate minerals.

The major and trace element concentration of black shale samples was respectively determined by X-ray fluorescence spectrometer (XRF, Primus II) and inductively coupled plasma mass spectrometer (ICP-MS, Agilent 7700e) at the Wuhan Sample Solution Analytical Technology Co., Ltd.

Before XRF analysis, all samples were dried at 105°C for 12 hours, and then no less than 5.0g of each sample was ashed at 815°C using a muffle furnace. The major elements oxides in the sample were determined by the melt plate method. Precision for determination of major elements oxides concentrations is better than 2.5%.

Prior to ICP-MS determination, each black shale sample was acid-digested according to the following process: Dry the samples at 105°C for 12 hours. 50 mg of each sample was digested with 1 ml HNO_3 and 1 ml HF, and heated at 190°C for more than 24 hours. Cool the digestion solution down, and evaporate it at 140°C on an electric heating plate until dry, then digest the residue with 1 ml HNO_3 and evaporate it to dry again. Thereafter, the residue was digested with1 ml HNO_3, 1 ml MQ water and 1 ml of internal standard In (the concentration is 1 μg/g) and heated at 190°C for more than 12 hours. Subsequently, the solution was diluted with 2% HNO_3 for ICP-MS determination. Multi-element standard sample (BHVO-2、BCR-2 and RGM-2) was used for calibration of trace element concentrations. Precision for determination of trace element concentrations is better than 5.0%.

4 Results

4.1 Mineralogical characteristics of black shales

Minerals in the Shuijingtuo black shales from the Luojiacun section are mainly composed of quartz and clay minerals, with small proportions of calcite, albite, clinochlore, and pyrite, as well as traces of siderite and gypsum (Table 1). Quartz is the most abundant mineral (21.1%-68.9%, avg. 43.0%) in the Shuijingtuo black shale. In some cases, quartz occurs with sharp edges and corners and large particles (Figure 2A), indicating a terrigenous origin (Dong et al., 2021; Chen et al., 2022; Ye et al., 2022; Gao et al., 2023). In other cases, quartz occurs as crystals of different sizes with better roundness, which is usually smaller than terrigenous quartz (Figures 2B, I), indicating an authigenic origin. The authigenic quartz was possibly formed from transformation of clay minerals, alteration of clastic minerals (feldspar, mica), dissolution of siliceous biological skeleton, pressure dissolution, or devitrification of volcanic ash (Zhang et al., 2018; Yan et al., 2021).

Illite is the primary clay mineral in the Shuijingtuo black shale (9.7%-52.3%, avg. 29.1% Table 1). Illite occurs in the form of long strips (Figures 2B, C) and pore infillings (Figures 2D, E). The former more likely indicated a terrigenous origin from shallow water shelf or slope sedimentary environment with low TOC content (Zhang et al., 2017). The latter was more likely to represent an authigenic origin, which was probably derived from the alteration of clastic feldspar minerals, the transformation of montmorillonite or mixed layer minerals, or from the precipitation of diagenetic solution (Zhang et al., 2018).

Carbonate minerals in the Shuijingtuo black shale mainly consist of calcite and dolomite, the content of which respectively ranges from 1.0% to 38.0% (avg. 10.8%) and from 1.1% to 6.0% (avg. 3.2%). Calcite

TABLE 1 Mineral composition and content of black shales of Shujingtuo Formation in Luojiacun, western Hubei Province (%).

Sample	Illite	Clinoch	Quartz	Calcite	Dolomite	Siderite	Pyrite	Gypsum	Albite
SJT-1	29.1	/	68.9	/	1.1	/	0.9	/	/
SJT-2	29.4	/	46.4	9.4	5.1	/	1.9	/	7.7
SJT-3	24.6	/	50.8	4.8	3.8	/	3.9	/	12.2
SJT-4	36.7	/	42.9	3.1	3.7	/	2.5	/	11.2
SJT-5	32.6	/	46.2	3.6	2.5	/	2.4	/	11.9
SJT-6	21.4	/	47.1	3.9	3.6	/	8.7	/	15.2
SJT-7	28.3	/	43.5	6.1	3.9	/	6.0	/	12.2
SJT-8	35.6	/	42.6	6.5	1.5	/	2.5	0.5	10.9
SJT-9	20.6	/	55.2	9.6	2.7	/	2.3	/	9.6
SJT-10	14.4	/	59.6	8.3	4.0	/	3.3	/	10.4
SJT-11	22.2	/	53.0	6.7	3.1	/	3.0	0.7	11.4
SJT-12	31.2	/	48.0	2.7	1.6	/	2.4	1.6	12.6
SJT-13	17.9	/	52.9	11.3	3.1	/	2.5	/	12.3
SJT-14	9.7	/	51.5	18.0	5.0	/	3.8	/	12.1
SJT-15	20.1	/	54.5	12.5	2.0	/	1.8	/	9.1
SJT-16	18.0	/	57.1	10.1	3.2	/	2.2	/	9.5
SJT-17	31.4	0.9	32.8	8.2	3.2	0.6	1.8	/	21.2
SJT-18	32.0	2.6	25.3	16.4	5.0	/	2.6	/	16.1
SJT-19	35.5	4.0	30.8	13.3	1.7	/	1.7	/	12.9
SJT-20	20.0	1.2	29.7	27.6	6.3	/	2.1	/	13.0
SJT-21	30.1	3.8	21.1	38.0	1.9	/	1.2	/	3.9
SJT-22	19.8	7.6	34.6	17.4	2.7	/	1.7	/	16.2
SJT-23	41.9	10.4	28.6	3.6	1.2	/	1.3	/	13.0
SJT-24	29.2	7.5	33.1	10.4	2.7	/	1.3	/	15.7
SJT-25	35.5	8.5	38.7	1.0	1.2	/	1.8	/	13.3
SJT-26	34.6	8.1	22.9	17.7	6.2	/	0.7	/	9.9
MIN	9.7	/	21.1	1.0	1.1	/	0.7	/	3.9
MAX	41.9	10.4	68.9	38.0	6.3	0.6	8.7	1.6	21.2
AVE	27.0	5.4	43.0	10.8	3.1	0.6	2.5	0.9	12.1

mostly exists in the form of fracture- or pore-infillings (Figures 2C, F), while dolomite mainly occurs as single crystals and calcareous cementation (Figure 2C), both indicating an authigenic formation process during the late diagenesis (Shao et al., 1998; Dai et al., 2015).

Pyrite is ubiquitously distributed in the Shuijingtuo black shale (0.7%-8.7%, avg. 2.5%). It mainly occurs in the form of single subhedral crystals (Figure 2H), and framboidal aggregate (Figure 2G), which is indicative of syngenetic origin (Chou, 2012). In a few cases, pyrite also occurs in the form of fracture infillings, filling in cracks of quartz and albite in granular or veinlet form during an epigenetic process (Figures 2A–C).

Albite is the primary feldspar mineral in the Shuijingtuo black shale (3.9%-21.2%, avg. 12.1%), which occurs in the form of long strips (Figure 2H) and subhedral crystals (Figures 2B–E), indicating terrigenous origin and an authigenic origin, respectively. In addition, phosphate minerals, e.g., apatite were also observed under the scanning electron microscope. Apatite is mainly present in the form of authigenic euhedral to subhedral particles (Figures 2A, I).

4.2 Geochemical characteristics of black shales

4.2.1 Major and trace element concentration

Based on the XRF analysis, SiO_2, Al_2O_3 and CaO are the predominant major element oxides in the Shuijingtuo black shale,

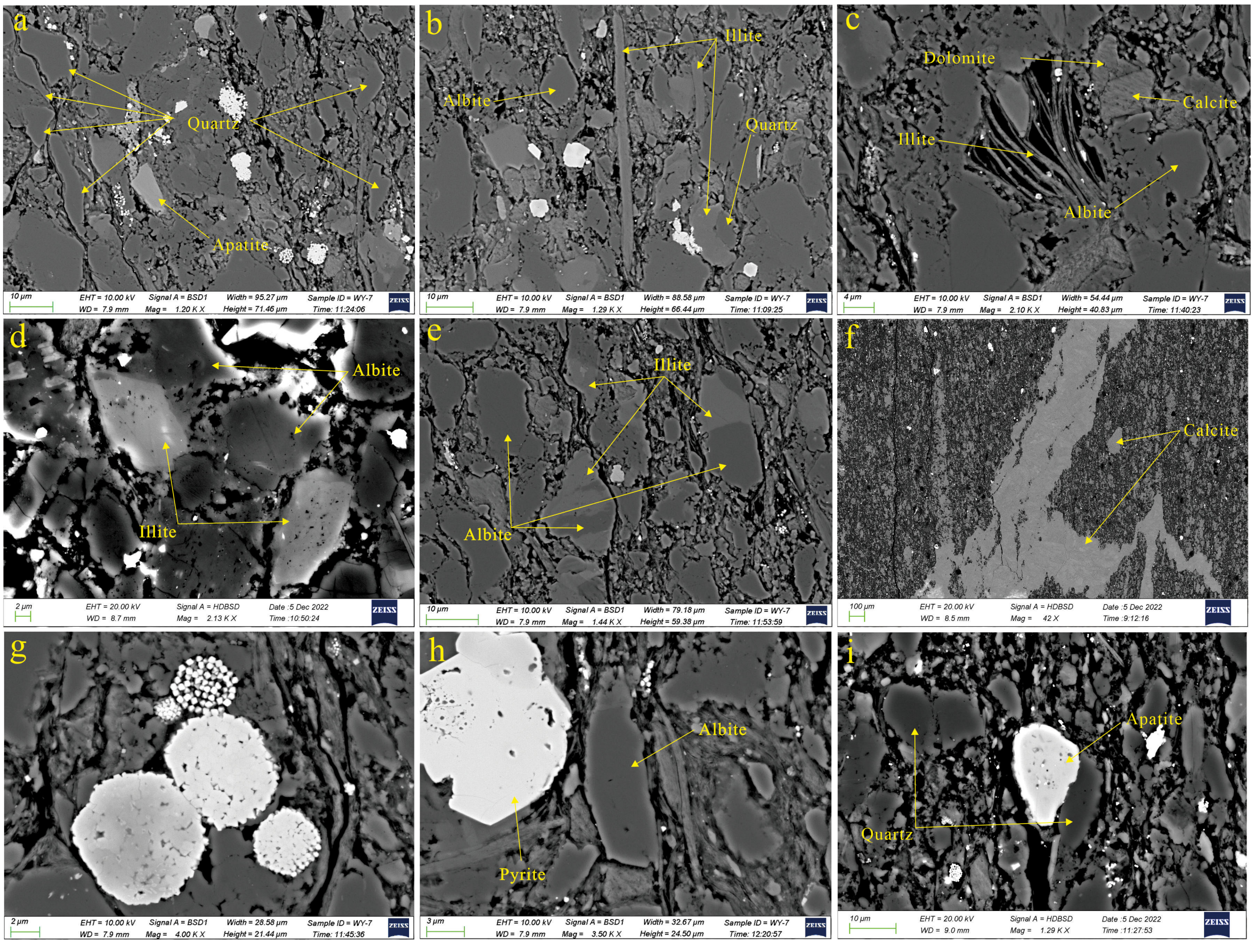

FIGURE 2
Modes of occurrence of minerals in the Shuiijingtuo black shale. **(A)** clastic quartz and apatite in sample No.7; **(B)** authigenic quartz, albite and illite in sample No.7; **(C)** illite, albite, calcite and dolomite in sample No.7; **(D)** authigenic illite and albite in sample No.9; **(E)** Mutually metasomatized illite and albite in sample No.7; **(F)** calcite vein in sample No.21; **(G)** framboidal pyrite in sample No.9; **(H)** single subhedral crystals pyrite and albite in sample No.7; **(I)** authigenic quartz, albite and apatite in sample No.7.

followed by Fe_2O_3, K_2O and MgO (Table 2). The content of SiO_2, Al_2O_3 and CaO varies from 37.3% to 65.2% (55.9%), 6.3% to 18.2% (avg. 10.3%), and 1.5% to 22.1% (avg. 8.2%), respectively. Secondarily, the content of Fe_2O_3, K_2O and MgO is respectively 2.3-6.0% (avg. 4.0%), 1.7-4.1% (avg. 2.8%), and 1.1-2.6% (avg. 1.8%). The content of other oxides (TiO_2, Na_2O, MnO and P_2O_5) is less than 1%. Compared with the major element oxide content of North American shale (NASC), CaO content of the Shuijingtuo black shale is slightly enriched (2.26 times higher), while the content of other major elements is similar or depleted. Compared with the average composition of post Archean Australian shale (PAAS), CaO content of the Shuijingtuo black shale is significantly enriched (6.25 times higher), and the content of other major elements is also similar or depleted. The elevated CaO content is ascribed to the relatively high calcite content of the Shuijingtuo black shale.

With respect to the trace elements in the Shuijingtuo black shale, their enrichment degree is evaluated by the concentration coefficient (CC) proposed by Dai et al. (2015). In order to eliminate the influence caused by the change of sedimentary rock composition, the Al-normalized concentration coefficient is used to quantify the enrichment degree of trace elements in this paper (McLennan, 2001a; Piper and Perkins, 2004; Li et al., 2017a, b, c), and the calculation formula is as follows: $CC=(X/Al)_{sample}/(X/Al)_{UCC}$, where X represents a given element in the sample and/or upper crust content (UCC). Compared with the trace element concentration in UCC (Taylor and McLennan, 1995), U is significantly enriched (CC>10), and Ba is enriched (5<CC<10) in the Shuijingtuo black shale (Supplementary Table 1; Figure 3). Uranium and Ba concentration respectively varies from 5.2 μg/g to 68.4 μg/g (avg. 32.4 μg/g) and 708 μg/g to 35156 μg/g (avg. 2846 μg/g). In addition, V, Cr, Ni and Sr are slightly enriched (2<CC<5), the concentration of which respectively ranges from 105 μg/g to 1446 μg/g (avg. 255 μg/g), 97.5 μg/g to 240 μg/g (avg. 165 μg/g), 38.2 μg/g to 216 μg/g (avg. 90.8 μg/g), and 155μg/g to 2583 μg/g (avg. 703 μg/g). The other trace elements (e.g., Li, Be, Sc, Co, Zn, Ga, Rb, Y, Zr, Nb, Sn, Cs, La, Ce, Pr, Nd, Hf, Ta, Tl, Pb and Th) in the Shuijingtuo black shale show similar or depleted concentrations compared to the average concentration of corresponding elements in UCC (CC<2).

The total concentration of rare earth elements (REE) in the Shuijingtuo black shale is 128 μg/g on average (80.9-201 μg/g)

TABLE 2 The content of major element in the blak shales of Shuingtuo Formation in Luojiacun, western Hubei Province (%).

Samples	SiO_2	TiO_2	Al_2O_3	Fe_2O_3	MnO	MgO	CaO	Na_2O	K_2O	P_2O_5	Al_2O_3/TiO_2
SJT-1	61.97	0.57	10.47	3.69	0.02	1.59	4.23	1.01	3.65	0.16	18.31
SJT-2	58.96	0.45	8.39	3.07	0.04	2.05	7.71	0.80	2.88	0.14	18.53
SJT-3	59.45	0.58	10.81	4.14	0.03	1.61	4.56	1.11	3.73	0.14	18.81
SJT-4	60.53	0.62	11.47	4.35	0.04	1.97	4.19	1.11	3.79	0.13	18.62
SJT-5	63.43	0.61	11.21	3.60	0.03	1.52	3.74	1.15	3.68	0.13	18.25
SJT-6	49.82	0.46	8.53	4.73	0.00	1.55	3.72	0.93	2.78	0.16	18.59
SJT-7	62.31	0.54	9.71	3.68	0.04	1.91	4.80	1.03	3.33	0.14	17.91
SJT-8	59.76	0.54	9.57	3.78	0.03	1.28	5.99	0.98	3.24	0.14	17.75
SJT-9	60.95	0.51	9.10	3.14	0.04	1.37	7.06	0.96	2.97	0.16	17.77
SJT-10	63.40	0.54	9.24	3.51	0.03	1.24	5.46	0.99	3.01	0.14	17.15
SJT-11	60.89	0.49	8.66	3.54	0.04	1.54	6.76	0.95	2.80	0.20	17.60
SJT-12	65.16	0.54	9.55	3.49	0.03	1.08	3.65	1.00	3.10	0.22	17.62
SJT-13	59.93	0.45	7.68	3.00	0.05	1.29	8.44	0.86	2.46	0.24	17.27
SJT-14	53.40	0.41	7.30	3.61	0.08	1.67	11.30	0.89	2.28	0.24	17.72
SJT-15	61.97	0.35	6.26	2.28	0.05	1.15	9.16	0.78	1.90	0.16	17.87
SJT-16	61.84	0.38	6.66	2.89	0.07	1.45	8.15	0.85	2.01	0.20	17.75
SJT-17	54.11	0.63	12.46	4.58	0.03	1.82	8.05	1.04	2.77	0.11	19.71
SJT-18	41.73	0.49	10.94	5.10	0.04	2.59	15.15	0.83	2.36	0.10	22.36
SJT-19	48.30	0.55	11.92	4.22	0.04	1.95	12.66	0.87	2.52	0.11	21.83
SJT-20	43.38	0.54	12.23	4.05	0.04	2.49	14.86	0.64	2.74	0.12	22.68
SJT-21	37.33	0.37	8.26	3.49	0.04	1.81	22.12	0.57	1.75	0.12	22.50
SJT-22	50.20	0.51	10.10	5.03	0.05	1.94	12.53	0.85	2.02	0.15	19.89
SJT-23	57.77	0.68	14.23	5.37	0.04	2.18	5.19	1.05	2.97	0.14	20.81
SJT-24	53.15	0.53	10.95	4.79	0.05	2.21	10.63	0.93	2.18	0.13	20.54
SJT-25	56.94	0.81	18.16	6.00	0.03	2.25	1.49	0.80	4.08	0.15	22.42
SJT-26	45.44	0.55	12.65	5.04	0.05	2.52	12.74	0.62	2.70	0.12	22.96
MIN	37.33	0.35	6.26	2.28	0.00	1.08	1.49	0.57	1.75	0.10	/
MAX	65.16	0.81	18.16	6.00	0.08	2.59	22.12	1.15	4.08	0.24	/
AVE	55.85	0.53	10.25	4.01	0.04	1.77	8.24	0.91	2.83	0.15	/
PAAS	63.7	1.01	19.2	7.33	0.1	2.24	1.3	1.21	3.8	0.16	/
NASC	64.9	0.70	16.9	5.67	0.1	2.86	3.6	1.14	4.0	0.13	/
$PASS_N$	0.88	0.52	0.53	0.55	0.35	0.79	6.25	0.75	0.75	0.95	/
$NASC_N$	0.86	0.75	0.61	0.71	0.64	0.62	2.26	0.80	0.71	1.16	/

(Supplementary Table 1), which is lower than that of the UCC (146.4 µg/g), NASC (160.1 µg/g) and PAAS (184.8 µg/g). The total concentration of light rare earth elements (LREE; e.g., La, Ce, Pr, Nd, Sm, Eu, Gd) and heavy rare earth elements (HREE; e.g., Tb, Dy, Ho, Er, Tm, Yb, Lu) respectively ranges from 73.3 µg/g to 190 µg/g (avg. 118 µg/g) and 7.2 µg/g to 14.1 µg/g (avg. 10.3 µg/g), accounting for 92% and 8% of the total REEs. The LREE/HREE ratio ranges from 9.5 to 16.1 (avg. 11.4), higher than that in NASC (9.7), indicating an enrichment of LREE in the Shuijingtuo black shale. Furthermore, according to the chondrite-normalized REE distribution pattern (Figure 4A), the LREE part shows an obvious rightward trend, while the HREE part shows a relatively flat slope, further indicating the high fractionation between LREE and HREE and the enrichment of LREE. When normalized to the REE values of NASC, the Shuijingtuo black shale presents a flat REE distribution pattern (Figure 4B), reflecting a consistent provenance and stable tectonic

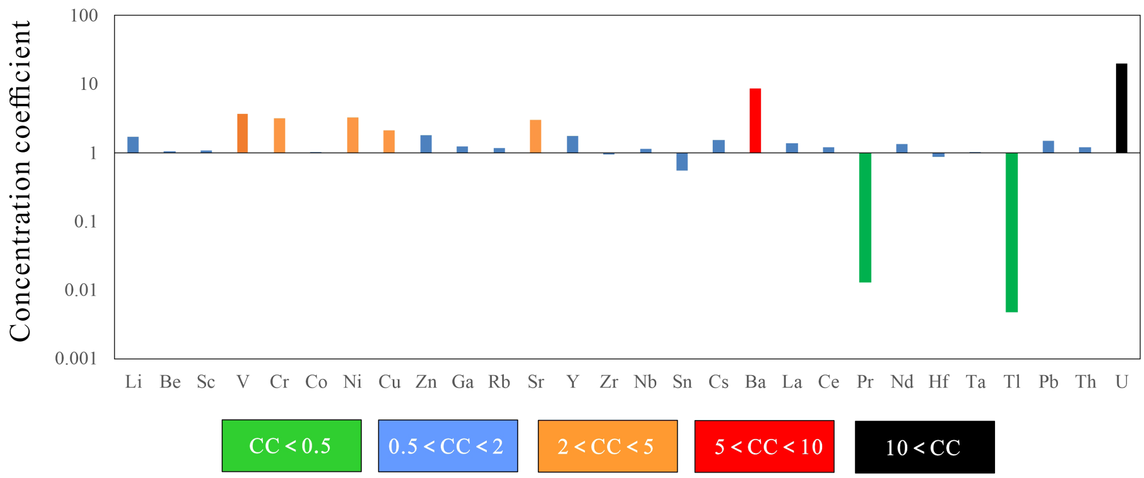

FIGURE 3
Concentration coefficients of trace elements in the Shuijingtuo black shale.

activity (Yan et al., 2021). The NASC-normalized $(La/Sm)_N$ value is 1.13 on average (0.94-1.5), representing a weak fractionation between light rare earth elements.

4.2.2 Distribution and modes of occurrence of elevated elements

According to unary linear regression method, the elevated V, Ni, U and Cr concentration have weak or negative correlation with Al_2O_3 content in the Shuijingtuo black shale (r= -0.07, -0.13, -0.61, -0.39) (Figures 5A–D). Furthermore, it is found that V, Ni, U and Cr concentrations present strong positive correlations with Si_{bio} content in the Shuijingtuo black shale (Figures 5E–H), which indicates that V, Ni, U, and Cr mainly occur in organic form in the Shuijingtuo black shale.

In addition, there is a strong positive correlation between Ba and pyrite in the Shuijingtuo black shale (Figure 5I), indicating that Ba is mainly hosted in pyrite. By contrast, a strong positive correlation between Sr and calcite in the Shuijingtuo black shale indicates that Sr is mainly hosted in calcite (Figure 6).

Vertically, the elevated V and Ni show similar variation characteristics, the contents of which are both higher in the upper portion of the Shuijingtuo black shale from the Luojiacun section (Figure 6). Chromium and U show similar vertical variation characteristics, the content of which are higher in the middle and upper section (Figure 6). Furthermore, Sr content is higher in the lower section and Ba content is higher in the middle section, which presents similar variation to calcite and pyrite content, respectively (Figure 6), furthering indicating the occurrence of Sr with calcite and Ba with pyrite.

5 Discussion

5.1 Tectonic environment

Through outcrop observation, core description, thin section observation, scanning electron microscope observation and geochemical analysis of main and trace elements, it is concluded that the Lower Cambrian sedimentary facies in the Middle Yangtze area is dominated by shallow water shelf - deep water shelf - slope sedimentary facies (Zhang et al., 2019; Zhao et al., 2019; Gao et al., 2020; Ding et al., 2021), among which the western Hubei - Hunan and Guizhou areas belong to deep water shelf - slope sedimentary facies (Zhao et al., 2019). Different tectonic environments have certain characteristics of provenance, and are characterized by specific sedimentary processes, which can be distinguished by several geochemical indexes. Sugisaki et al. (1983) pointed out that the MnO/TiO_2 ratio can be effectively used to distinguish the tectonic environment, with value of 0.5 ~ 3.5 and <0.5 indicative of a deep-sea or trench ocean bottom environment far away from the continent, and a nearshore shallow sea or continental slope environment, respectively. The MnO/TiO_2 ratios of the Shuijingtuo black shale samples range from 0.03 to 0.19 (avg. 0.08), reflecting a nearshore shallow sea or continental slope environment.

Murray (1994) proposed the discrimination diagram of $Al_2O_3/(Al_2O_3+TFe_2O_3)$ - TFe_2O_3/TiO_2 to reflect tectonic environment, in which all the Shuijingtuo black shale samples fall into the continental margin environment (Figure 7A). In the diagram of $Al_2O_3/(Al_2O_3+TFe_2O_3)$ - $(La/Ce)_N$, all the Shuijingtuo black shale samples fall within the continental margin environment as well (Figure 7B). Moreover, the δCe value also can accurately distinguish three tectonic environments near the mid ocean ridge, the pelagic basin and the continental margin. Zhou (2019) proposed that the δCe value of 0.18-0.38, 0.51 ~ 0.61 and 0.74 ~ 0.96 respectively indicates a regional sedimentation near the ocean ridge, the pelagic basin, and the continental margin, and found that the Niutitang (corresponding to the Shuijingtuo) black shale in Northwest Hunan was formed in the deep- to semi deep-water sedimentary environment close to the continental margin. The δCe values of the Shuijingtuo black shale samples in this study range from 0.82 to 1.00 (avg. 0.94), also indicating the normal continental margin environment. Furthermore, SiO_2-log (K_2O/Na_2O) diagram also can

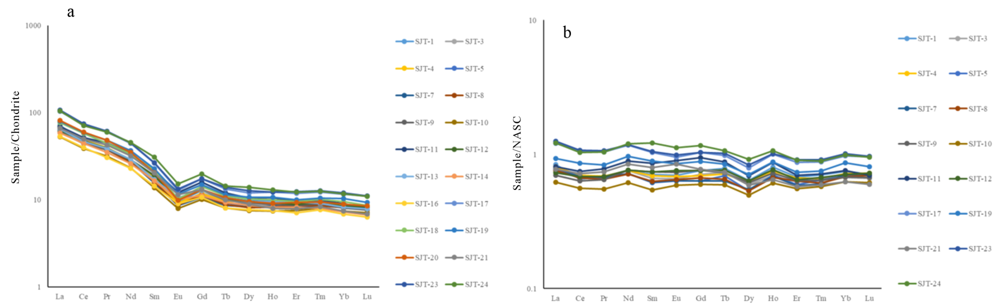

FIGURE 4
REE distribution patterns with chondrite standard **(A)** and NASC standard **(B)** for the Shuijingtuo black shale.

be used to identify the tectonic environment (Roser and Korsch, 1986; Huang et al., 2013). In the diagram of SiO_2-log (K_2O/Na_2O), all the Shuijingtuo black shale samples fall within the passive continental margin (Figure 7C). The normal continental margin includes shallow sea shelf and semi-deep sea slope, which is consistent with the founding that the tectonic location of the Luojiacun profile belongs to shelf margin - upper slope area (Hu, 2019).

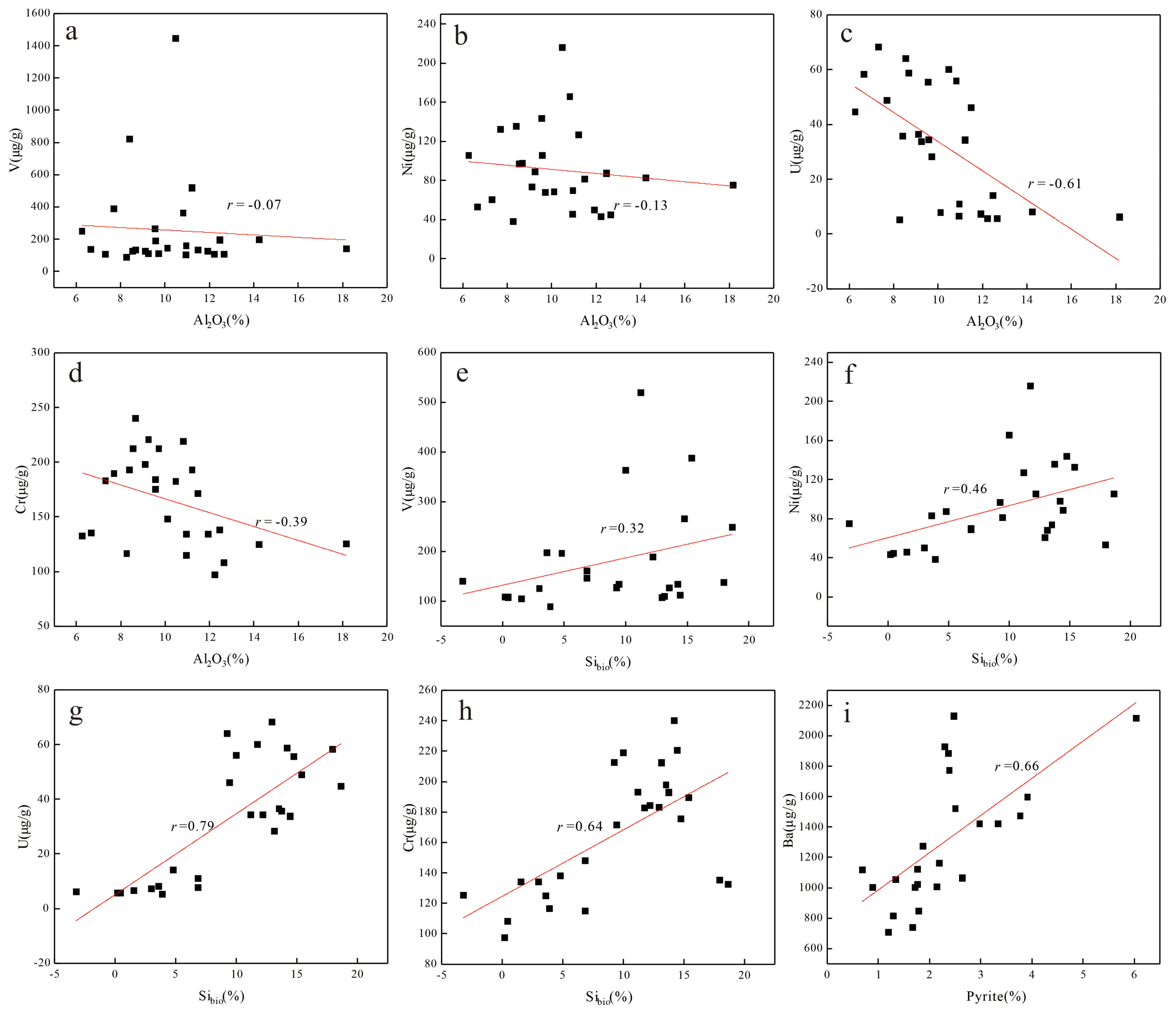

FIGURE 5
Occurrence modes of elevated elements in the Shuijingtuo black shale. **(A)** V vs. Al_2O_3; **(B)** Ni vs. Al_2O_3; **(C)** U vs. Al_2O_3; **(D)** Cr vs. Al_2O_3; **(E)** V vs. Si_{bio}; **(F)** Ni vs. Si_{bio}; **(G)** U vs. Si_{bio}; **(H)** Cr vs. Si_{bio}; **(I)** Ba vs. Pyrite.

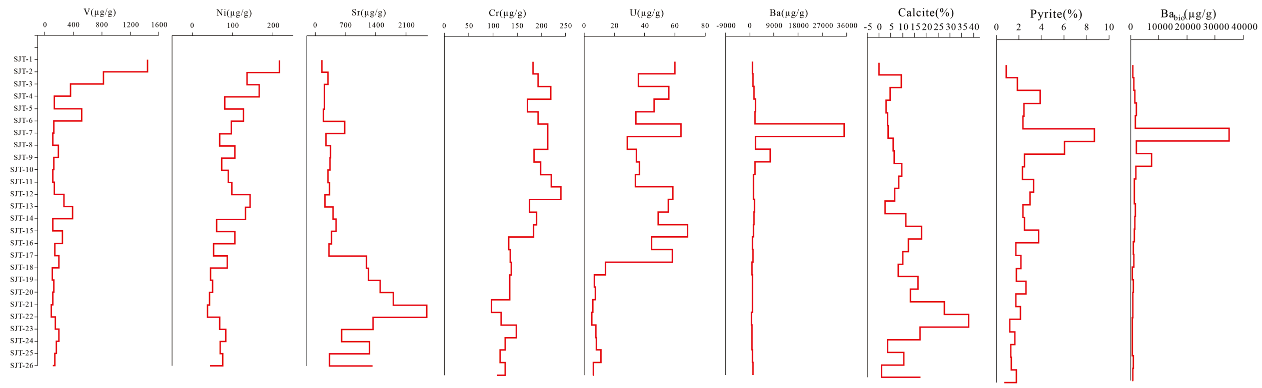

FIGURE 6
Vertical characteristics of enriched trace elements in the Shuijingtuo black shale.

5.2 Sediment provenance

Generally, provenances from sediment source region, marine biological precipitation/recrystallization, and volcanic ash are the dominant sources for black shales and other sediments. The input of terrigenous clastic materials can be manifested by contents and ratios of some elements that are not easily affected by diagenesis and weathering process (Murray, 1994; Murphy et al., 2000; Rachold and Brumsack, 2001; Rimmer, 2004; Tribovillard et al., 2006; Calvert and Pedersen, 2007; Lézin et al., 2013). According to the discriminant indicators of Ti/Al, Th/Al and Zr/Al ratios, the terrigenous clastic input of the Shuijingtuo black shale was of medium degree and remained relatively stable during the deposition process (Yang, 2020). The Al_2O_3/TiO_2 ratio was also widely used as an efficient indicator of the source rock composition, with 3-8, 8-21, and 21-70 respectively of mafic basalt, intermediate

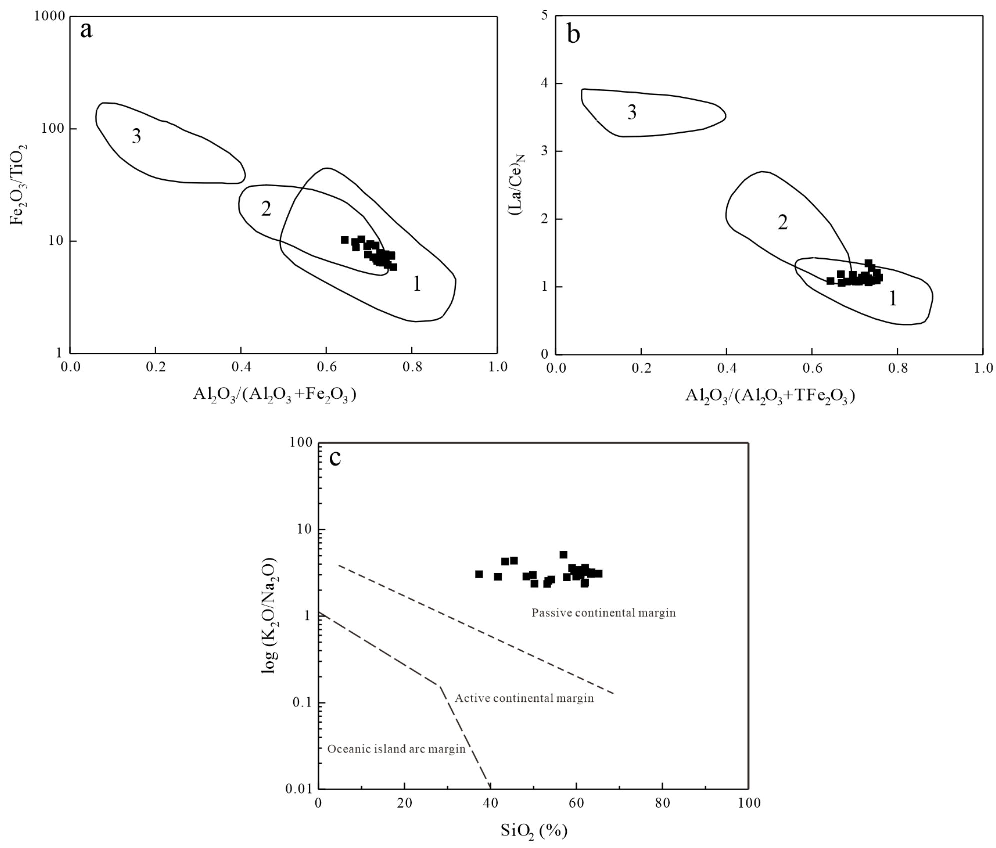

FIGURE 7
Tectonic environment discrimination of Shuijingtuo black shales. **(A)** Diagram of Fe_2O_3/TiO_2 vs. $Al_2O_3/(Al_2O_3+Fe_2O_3)$; **(B)** $(La/Ce)_N$ vs. $(Al_2O_3+TFe_2O_3)$; **(C)** $\log(K_2O/Na_2O)$ vs. SiO_2. 1-Continental margin; 2-Pelagic Basin; 3-Mid-oceanic ridge.

granodiorite, and felsic granite source (Hayashi et al., 1997). The Al_2O_3/TiO_2 ratios of the Shuijingtuo black shale in Luojiacun section range from 17.2 to 23.0 (avg. 19.4), predominantly falling within the field of intermediate granodiorite (Figure 8A), which indicates that the terrigenous material source for the Shuijingtuo black shales is of intermediate granodiorite composition. In addition, the TiO_2/Zr ratio of >200, 55-199, and <55 respectively represents a mafic, intermediate, and felsic igneous source rock (Hayashi et al., 1997). The TiO_2/Zr ratios of the Shuijingtuo black shale samples ranges from 38.6 to 56.4, with an average of 44.9, manifesting that the sediment source for the study area is primarily of intermediate to felsic composition (Figure 8B). Moreover, the La–Th–Sc ternary diagram and cross plots of Th/Sc versus Zr/Sc, and La/Th vs. Hf are also reliable indicators of source rock composition (McLennan, 2001b; Vosoughi Moradi et al., 2016; Zhai et al., 2018), according to which the Shuijingtuo black shale samples primarily fall within the field close to felsic and granodiorite source (Figures 8C–E). Based on all these geochemical indexes, it is concluded that the Shuijingtuo black shale from the Luojiacun section were predominantly sourced from intermediate to felsic rocks similar to granodiorite.

Apart from the terrigenous supply, marine biogenic production also contributes as a provenance of the Shuijingtuo black shale from the Luojiacun section. Element Si is often used to reflect the input degree of terrigenous clasts (Murphy et al., 2000; Tribovillard et al., 2006), because Si is generally preserved in quartz and silicate minerals derived from terrigenous clasts (Kidder and Erwin, 2001). However, many studies have shown that marine sediments are usually rich in biogenic silica. The Si/Al ratio of the Shuijingtuo black shale samples ranges from 2.76 to 8.73 (avg. 5.10), which is higher than the average value of terrigenous sediment (3.11, Wedepohl, 1991). This indicates that the excessive Si and the occurrence of authigenic quartz (Figures 2B, I) in the Shuijingtuo black shale may be caused by biogenesis other than terrigenous input (Wojcik-Tabol and Slaczka, 2009). Previous research has also revealed that the provenance for the Early Cambrian black shales in the Yangtze platform was strongly influenced by the marine biogenic production (Wu et al., 2016; Zhu et al., 2021; Xia et al., 2022; Wang et al., 2023; Fu et al., 2023b).

5.3 Palaeoredox conditions

The Palaeoredox environment plays a crucial role in the distribution and evolution of marine organisms, as well as in the circulation, differentiation and enrichment of elements in marine sediments (Chang et al., 2009). It has been confirmed by several research that the early Cambrian black shales in the Yangtze Platform were deposited under an anoxic palaeoredox conditions (Xu et al., 2013; Han et al., 2015; Wu et al., 2016; Zhu et al., 2021; Xia et al., 2022; Wang et al., 2023; Fu et al., 2023b). Correspondingly, several redox sensitive elements and elemental ratios are useful indicators of palaeomarine environment, especially the palaeoredox conditions (Wignall, 1994; Crusius et al., 1996; Algeo, 2004; Algeo and Maynard, 2004; Rimmer, 2004; Rimmer et al., 2004; Tribovillard et al., 2004; Abanda and Hannigan, 2006; Tribovillard et al., 2006; Zhang et al., 2023). For instance, V/(V+Ni) ratio of >0.84, 0.54-0.82, and <0.60 respectively reflects euxinic, anoxic, and dysoxic to oxic conditions, and U/Th ratio of >0.5 is generally indictive of anoxic condition (Jones and Manning, 1994). The U/Th and V/(V+Ni) ratios of the Shuijingtuo black shale samples vary from 0.37 to 10.50 (avg. 4.31) and 0.56 to 0.87 (avg. 0.69), respectively, mostly falling

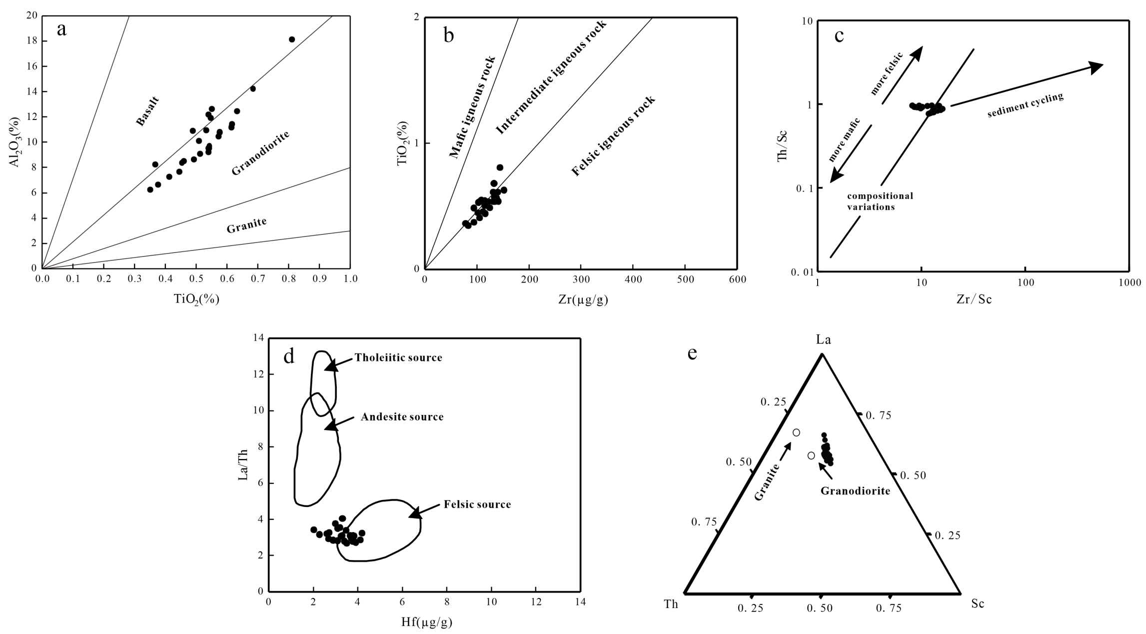

FIGURE 8
Source rock composition of the Shuiijingtuo black shales. **(A)** Cross plots of Al_2O_3 versus TiO_2; **(B)** Cross plot of TiO_2 and Zr; **(C)** Cross plot of Th/Sc versus Zr/Sc; **(D)** La/Th versus Hf bivariate plot; **(E)** La-Th-Sc diagram for the Shuijingtuo black shales.

within the anoxic field in the cross plots of V/(V+Ni) vs. U/Th (Figure 9), indicate that the Shuijingtuo black shale was primarily deposited under anoxic to euxinic conditions. Similarly, Ni/Co ratio of >7, 5-7, and <5 respectively reflects anoxic, dysoxic, and oxic conditions (Jones and Manning, 1994). The Ni/Co ratio of the Shuijingtuo black shale samples vary from 3.24 to 16.62 (avg. 8.18), also indicating deposition of the Shuijingtuo black shale under anoxic conditions.

Furthermore, authigenic uranium ($U_a=U_{total}$-Th/3) and δU (δU=U/[1/2 (U+Th/3)]) are also commonly used to refer the palaeoredox conditions of sedimentary environment (Wignall, 1994; Wignall and Myers, 1998). The U_a content of less than 5 μg/g generally indicates an oxidizing condition (Jones and Manning, 1994), while δU>1 and <1 respectively indicates an anoxic and normal marine sedimentary environment (Wignall, 1994). The U_a and δU of the Shuijingtuo black shale respectively ranges from 0.6 to 66.2 μg/g (avg. 29.5 μg/g), and 1.05 to 1.94 (avg. 1.68), further manifesting an anoxic sedimentary environment of the Shuijingtuo black shale.

Studies on Ce anomalies in modern seawater show that Ce is a sensitive factor for judging the redox environment (Yang et al., 2008). Generally, under oxidation conditions, Ce^{3+} is oxidized to Ce^{4+}, Ce^{4+} is prone to hydrolysis and precipitation by adsorption of Fe and Mn oxides, which is separated from other rare earth elements, resulting in Ce depletion in seawater. Under anoxic reduction conditions, Fe oxides dissolve and Ce^{4+} is reduced to Ce^{3+}, resulting no obvious Ce anomaly in seawater. Consequently, the variation of δCe value reflects the reduction-oxidation variation of sedimentary environment (DeBaar et al., 1985), and the δCe value of 0.78 is used as the reference value to discriminate the redox conditions of depositional environment (Wright et al., 1987). Coincident with those concluded from the above-mentioned geochemical indexes, the δCe of the Shuijingtuo black shale samples is between 0.82 and 1.00 (avg. 0.94), indicating a relatively anoxic environment as well.

A set of black shales with high organic matter was deposited in the Ordovician-Silurian, and its depositional environment was also anoxic-reductive (Mustafa et al., 2015; Mohammed et al., 2020; Zhou et al., 2021; Yi et al., 2022; Fu et al., 2023a), which is consistent with the depositional environment of the Shuijingtuo Formation in this paper. These results indicate that the shales with high organic matter have a positive correlation with the anoxic environment, which can provide indications for shale gas exploration and paleoenvironmental restoration.

5.4 Palaeomarine productivity

It is widely accepted that apatite is closely related to biological life activities, and has two kinds of formation mechanism. The first is the direct action of biology (Li et al., 2017a), that is, through biological life activities, the dispersed phosphorus in the medium is absorbed and formed into phosphate shell or bone, which is preserved in sediments after biological death, and transformed into apatite during diagenesis. The apatite formed by this mechanism is bioclastic apatite. The second is the indirect effect of biology, which is mainly affected by biomass and redox conditions. The indirect effect of biology is the main form of apatite formation in the early Cambrian. Al_2O_3 is generally considered in geochemistry to be derived only from terrigenous

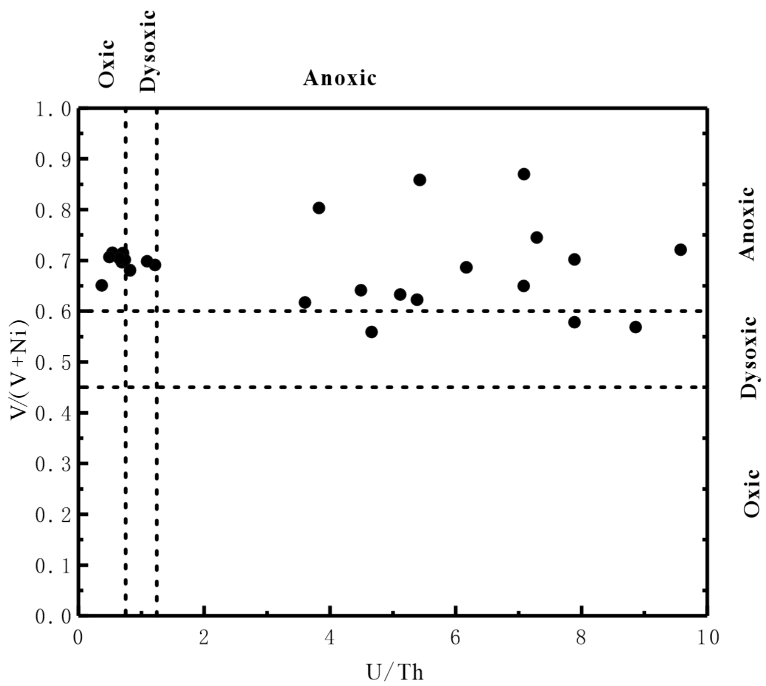

FIGURE 9
Cross plots of U/Th versus V/(V+Ni) of the Shuijingtuo black shale.

clastic inputs (Liu, 2017; Li et al., 2017a). According to unary linear regression method, there is a significant negative correlation between P_2O_5 and Al_2O_3 (Figure 10A), and an obvious positive correlation with TOC (Figure 10B) in the black shale of the Shuijingtuo Formation. Although P is not enriched in the black shale of the Shuijingtuo Formation (Table 2), P is still biogenic and related to higher palaeomarine productivity.

In addition, the content of biological silicon (Si_{bio}) can be used to restore palaemarine productivity, which is quantified by the following formula (Murray and leinen, 1996): $Si_{bio}=Si_{sample} - [(Si/Al)_{average\ shale} \times Al_{sample}]$, where Si_{sample} and Al_{sample} are the total Si and Al content in the studied sample, $(Si/Al)_{average\ shale}$ (3.11) is the Si/Al ratio of average shale (Taylor and Mclennan, 1985). The Si_{bio} content of the Shuijingtuo black shale samples is 9.2% on average, accounting for 35.5% of the total Si. Moreover, the Si_{bio} of the Shuijingtuo black shale is obviously correlated with the TOC (Figure 10I), which is in consistence with previous study that biogenic silicon in marine shale is usually highly correlated with organic carbon content (Luo et al., 2013). The main source of biogenic silicon is various siliceous plankton, such as diatoms, radiolarians and sponge spicule (Aplin and Macquaker, 2011), which is also the primary source of organic matter in marine sediments. The prosperity of plankton is usually accompanied by high organic matter (total organic carbon) content, both of which are responsible for the high paleo productivity. The primary productivity of the Shuijingtuo black shales is relatively high (TOC=1.9-6.5%, avg. 3.9%), manifesting the contribution of biogenic production to black shales.

Furthermore, the element Ba is widely used as a credible indicator for primary productivity of paleo ocean (Dehairs et al., 1987; Dymond et al., 1992; Paytan et al., 1996; Eagle et al., 2003; Tribovillard et al., 2006). The sources of barium in sediments mainly include biogenic barium, barium from terrestrial aluminosilicates, the precipitation of submarine hydrothermal barium and the secretion of some benthic organic organism (Dymond et al., 1992; Gonneea and Paytan, 2006). Only biogenic barium can reflect palaeoproductivity. Barium from biological sources is mainly precipitated in sediments in the form of barium

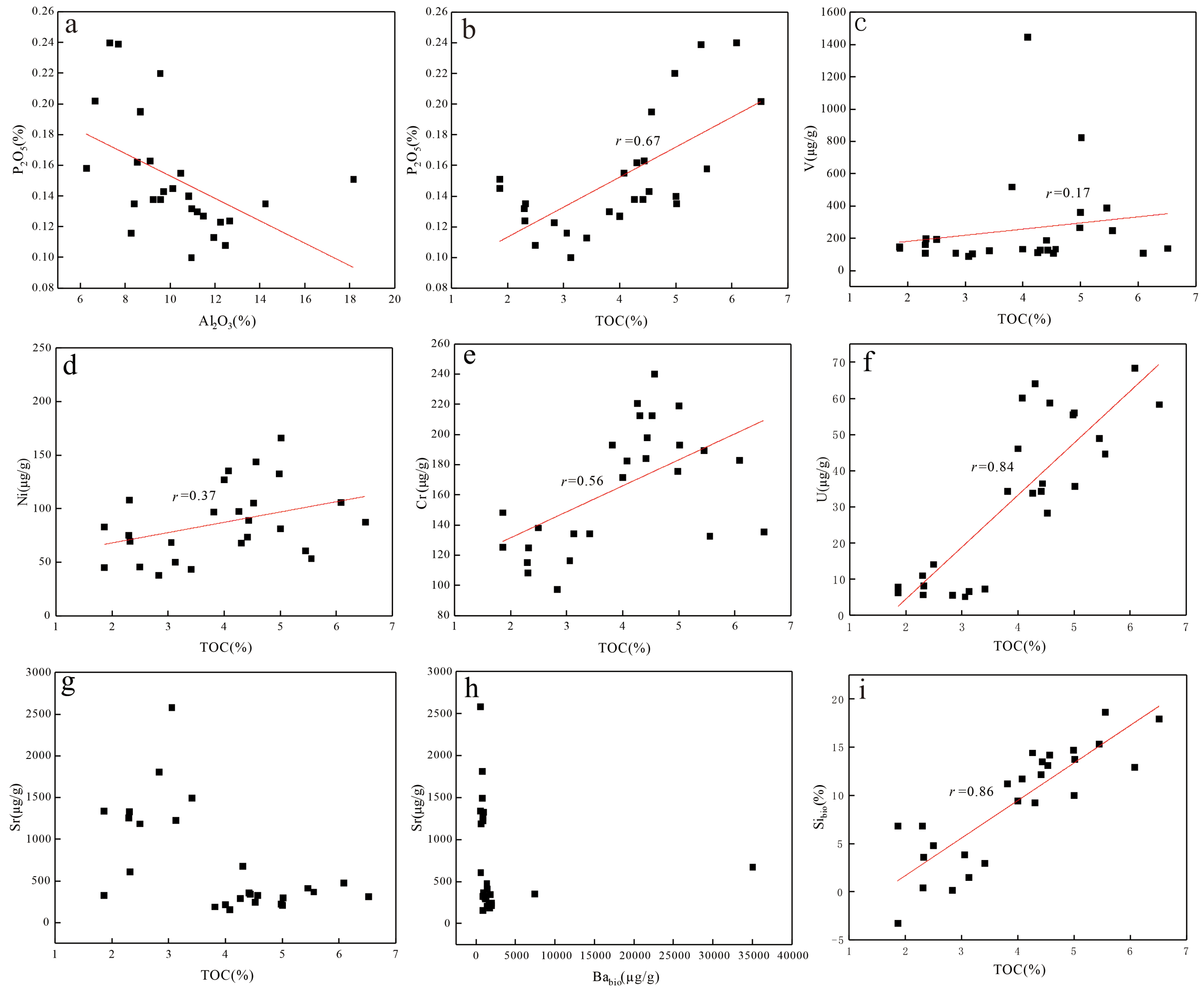

FIGURE 10
Cross plots of P_2O_5 versus Al_2O_3 **(A)** and TOC **(B)**; **(C-F)** TOC versus elevated elements; Sr versus TOC **(G)** and Ba_{bio} **(H)**; **(I)** Si_{bio} versus TOC of the Shuijingtuo black shales.

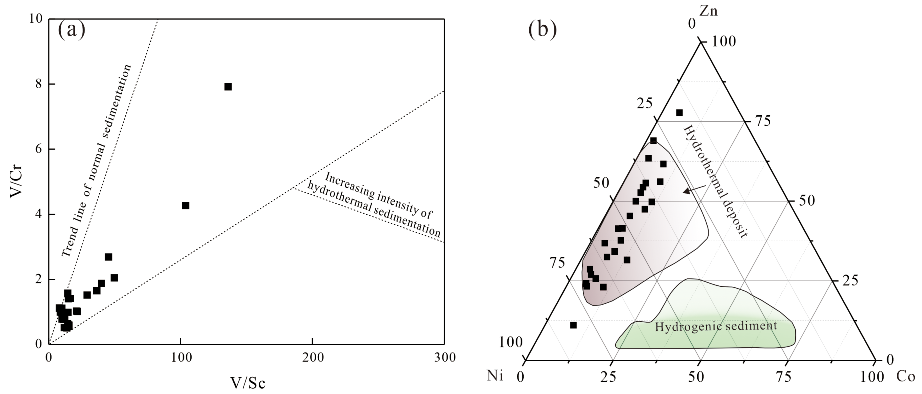

FIGURE 11
(A) Cross plot of V/Cr versus V/Sc; **(B)** Ni-Co-Zn three-phase diagram of the Shuijingtuo black shale.

sulfate (Barite). For the genesis of barium sulfate crystals, the current mainstream view is that there are some SO_4^{2-} ions on the surface of organic matter in the reduction microenvironment of marine diatom cell membrane and some particles, and Ba^{2+} in water will combine with them to form barium sulfate, which will then be deposited on the ocean floor. There is a positive correlation between the amount of barium sulfate crystal precipitation and the amount of organic matter, so the higher the Ba content in the sediment, the higher the primary productivity of the ocean surface.

Currently, it is universally acknowledged that the content of biogenic barium in sediments is 1000 ~ 5000 µg/g, indicating that the Palaeocean surface productivity is high (Murray and Leinen, 1993; Schoepfer et al., 2015). The specific calculation formula is $Ba_{bio}=Ba_{sample} - Al_{sample} \times (Ba/Al)_{clasts}$, where Ba_{sample} and Al_{sample} are the total Ba and Al content in the studied sample, respectively, and $(Ba/Al)_{clasts}$ are the average Ba/Al ratio of crustal rocks (0.0032-0.0046, Taylor and Mclennan, 1985). In this study, the $(Ba/Al)_{clastics}$ value is taken as 0.0032 to calculate the Ba_{bio} content of the Shuijingtuo black shale samples. The Ba_{bio} content of Shuijingtuo black shale samples in Luojiacun profile range from 568 to up to 35011 µg/g (avg. 2672 µg/g), also indicating that the primary productivity of Shuijingtuo black shale in Luojiacun profile is high. The high primary productivity of Shuijingtuo black shale in Luojiacun profile is also consistent with the previous studies (Wu et al., 2016; Zhu et al., 2021; Xia et al., 2022; Wang et al., 2023; Fu et al., 2023b).

5.5 Enrichment mechanism of elevated critical elements

Several productivity- and redox-sensitive elements, such as V, Ni, U, Cr, and Ba have been found enriched in the Shuijingtuo black shale (Yang and Yi, 2012). In the current study, the Shuijingtuo black shale from the Luojiacun section is significantly enriched in U, and enriched in Ba, V, Cr, Ni and Sr.

As stated above, the terrigenous provenance of the Shuijingtuo black shale is primarily of intermediate to felsic composition. However, the contents of U, V, Cr, and Ni in intermediate and felsic rocks are much lower than those in basic and ultrabasic rocks (Vinogradov, 1986), with U, V and Cr content in felsic rocks of 3.5µg/g, 18µg/g, and 8µg/g respectively (Vinogradov, 1986; Condie, 1993). Therefore, the enrichment of these elements in the Shuijingtuo black shale is not ascribed to the intermediate to felsic terrigenous provenance.

Murphy et al. (2000) have found that the strong anoxic condition and slow deposition is responsible for the enrichment of some trace elements, especially those redox sensitive ones in the nutrient-rich upwelling area. Redox sensitive elements such as V, Ni and Cr are prone to enrichment under anoxic conditions in the early diagenetic stage, due to that these redox sensitive elements are generally insoluble and precipitated into insoluble phases under anoxic/euxinic conditions (Sadiq, 1988; Tribovillard et al., 2006). Because the uranium content in open oceans, rivers and upper continental crust is very low, authigenic uranium under anoxic conditions is the main source of uranium in marine sediments. Under anoxic environment, uranium will diffuse in water and deposit in oxygen poor layer to form organometallic ligands and metal complexes (Algeo and Maynard, 2004; Tribovillard et al., 2012). As discussed above, the elevated V, Cr, U, and Ni in the Shuijingtuo black shale show the vertical distribution characteristics (Figure 6). Moreover, V, Ni, Cr, and U have a close correlation with TOC (r=0.17-0.84; Figures 10C–F), indicating that the enrichment of these elements in the black shale is closely related to organic matter by means of complex interaction process under the reduction environment, which needs further investigation.

In addition, the abnormal enrichment of V-Cr-Ni-U element assemblages in organic-rich rocks, e.g., coal and black shale, is often related to hydrothermal activities (Dai et al., 2013a; Jia, 2018). The submarine hydrothermal activity is due to the uplift of the continental crust, which contributes to the intrusion of underground magma along the weak zone, carrying a high content of metal elements into the sedimentary water body. On one hand, the influx of Mo, Ni, U and other elements will form a heavy metal mineral layer in the seawater. On the other hand, the increase of Fe, P and other life elements will provide sufficient nutrients for aquatic organisms, promote the growth of organisms, and produce higher primary productivity. Furthermore, the occurrence of hydrothermal activities will also locally change the redox conditions of water bodies. A large number of Fe and Mn elements enter the water bodies, forming an H_2S rich anoxic reduction environment at the bottom, resulting in the enrichment of some trace elements (Morforda et al., 2001). Hydrothermal sedimentation will also promote the migration and accumulation of trace elements in sedimentary rocks.

In the current research, the hydrothermal activities is evidenced by geochemical indexes, such as V/Sc and V/Cr ratios, which can be used to distinguish hydrothermal source from normal authigenic element deposition (Yang, 2020). Sc/Cr ratio of <0.120 and >0.144 indicates a hydrothermal sedimentation and normal seawater sedimentation, respectively, while Sc/Cr ratio between 0.120 and 0.144 represents the joint influence of normal seawater sedimentation and hydrothermal sedimentation (Yang, 2020). The Shuijingtuo black shale samples in Luojiacun profile predominantly fall between the trend line of normal sedimentation and the hot water sedimentation line, indicating that the Shuijingtuo black shale was affected by hydrothermal sedimentation (Figure 11A). Additionally, Zn, Ni, Cu and other elements are often enriched due to submarine hydrothermal activities in seawater, while Co is mainly derived from hydrogenic sedimentary environment (Choi and Hariya, 1992). Therefore, the Ni-Co-Zn three-phase diagram is usually used to trace the hydrothermal (Choi and Hariya, 1992). In the Ni-Co-Zn three-phase diagram, the overwhelming majority of the Shuijingtuo black shale samples fall within Hydrothermal deposit area (Figure 11B), further indicating that the Shuijingtuo black shale was affected by hydrothermal sedimentation. Furthermore, calcite is filled in the fracture in the form of veins (Figure 2F), also is an indication of the hydrothermal sedimentation of the Shuijingtuo Formation black shale. Because Luojiacun section was deposited in deep-water continental shelf area, the hydrothermal activity during the deposition process was submarine hydrothermal deposition. Consequently, the submarine hydrothermal fluid accompanying the anoxic condition, high palaeomarine productivity are responsible for the enrichment of U, V, Ni, and Cr in the Shuijingtuo black shale (Figure 12).

With respect to the enrichment of Ba, it is accepted that biogenic process can to some extent give rise to the enrichment of some elements (e.g., Cu, Zn and Ba) by marine organism activity (Breit and Wanty, 1991; Luning et al., 2000; Brumsack, 2006; Tribovillard et al., 2006; Yan et al., 2015; Zhao et al., 2016; Smolarek et al., 2017). The Shuijingtuo black shale of Luojiacun section is characterized by high primary productivity, and occurrence of elevated biological Ba, which indicates that Ba enrichment in Shuijingtuo black shale is mainly the result of higher primary productivity. However, there is no correlation between Sr and TOC (Figure 10G) and Ba_{bio} (Figure 10H) in the Shuijingtuo Formation black shale, indicating that the enrichment of Sr is not related to the biological combination and primary productivity, but mainly related to the anoxic-euxinic sedimentary environment.

6 Conclusion

The Shuijingtuo black shale from the Luojiacun section, Western Hubei Region is characterized by high TOC content and enriched in V-Cr-Ni-U and Sr-Ba elevated critical element assemblages. The elevated V, Cr, Ni, and U present organic affinities, which primarily occur in organic matter in the Shuijingtuo black shale. Strontium is closely correlated to calcite and Ba is closely correlated to pyrite.

The Shuijingtuo black shale was deposited in anoxic conditions in nearshore shallow sea or continental slope environment close to the continental margin, and has a high palaeomarine productivity. Terrigenous provenance of the Shuijingtuo Formation in Luojiacun section is mainly medium-feldspathic granodiorite, which is not

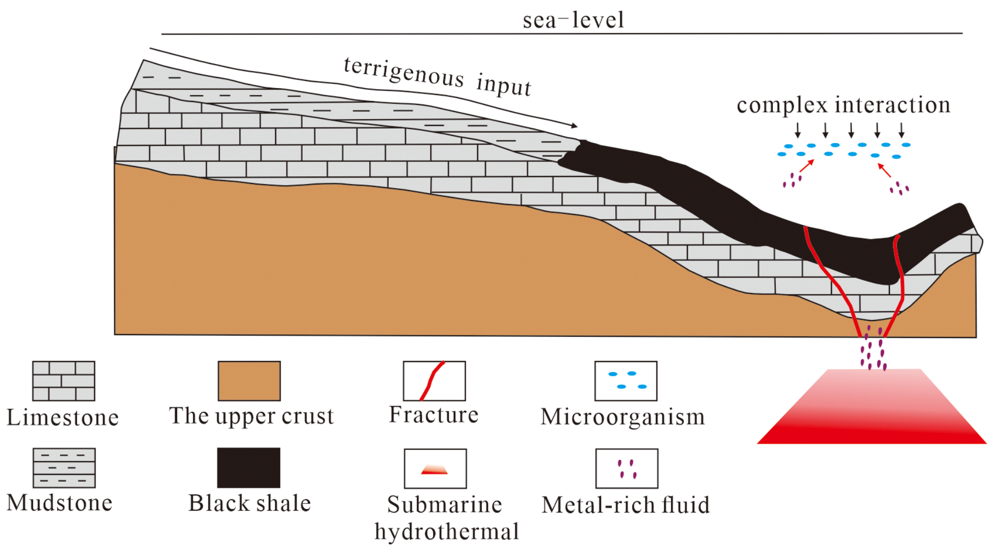

FIGURE 12
Enrichment pattern of elevated elements.

responsible for the enrichment of V-Cr-Ni-U and Sr-Ba critical element assemblages in Shuijingtuo black shale.

The enrichment of U, V, Cr, and Ni in the Shuijingtuo black shale is ascribed to the anoxic condition, high palaeomarine productivity and the submarine hydrothermal solutions. Barium enrichment is predominantly caused by higher primary productivity, while Sr enrichment is primarily ascribed to anoxic depositional conditions.

Data availability statement

The original contributions presented in the study are included in the article/Supplementary Material. Further inquiries can be directed to the corresponding author.

Author contributions

YW: Resources, Writing – original draft, Methodology, Investigation, Conceptualization. JL: Writing – review & editing, Resources, Project administration, Data curation, Conceptualization. YL: Writing – review & editing, Validation. XGZ: Writing – review & editing, Validation. VH: Writing – review & editing. PW: Writing – review & editing. XL: Writing – review & editing, Resources, Investigation. HZ: Writing – review & editing, Resources, Investigation. XYZ: Writing – review & editing, Resources, Investigation.

Funding

The author(s) declare that financial support was received for the research, authorship, and/or publication of this article. This research was funded by the National Key R&D Program of China (No. 2021YFC2902000), the Third Xinjiang Scientific Expedition Program (No. 2023xjkk0100), the Natural Science Foundation of China (Nos. 42372199 and 41972179), the Key State Science and Technology Project of Xinjiang Uygur Autonomous Region (No. 2022A03014-2) and the Foreign Experts Program for The Belt and Road Innovative Talent Exchange (No. DL2023155001L). The authors express great gratitude to the editor and anonymous reviewers for their comments, which greatly improved the manuscript quality.

Conflict of interest

The authors declare that the research was conducted in the absence of any commercial or financial relationships that could be construed as a potential conflict of interest.

Publisher's note

Supplementary material

The Supplementary Material for this article can be found online at: https://www.frontiersin.org/articles/10.3389/fmars.2024.1457964/full#supplementary-material

References

Abanda, P. A., and Hannigan, R. E. (2006). Effect of diagenesis on trace element partitioning in shales. *Chem. Geol.* 230, 42–59. doi: 10.1016/j.chemgeo.2005.11.011

Algeo, T. J. (2004). Can marine anoxic events draw down the trace element inventory of seawater? *Geology* 32, 1057–1060. doi: 10.1130/G20896.1

Algeo, T. J., and Maynard, J. B. (2004). Trace-element behavior and redox facies in core shales of Upper Pennsylvanian Kansas-type cyclothems. *Chem. Geol.* 206, 289–318. doi: 10.1016/j.chemgeo.2003.12.009

Algeo, T. J., and Rowe, H. (2012). Paleoceanographic applications of trace-metal concentration data. *Chem. Geol.* 324-325, 6–18. doi: 10.1016/j.chemgeo.2011.09.002

Aplin, A. C., and Macquaker, J. (2011). Mudstone diversity: Origin and implications for source, seal, and reservoir properties in petroleum systems. *AAPG Bull.* 95, 2031–2059. doi: 10.1306/03281110162

Armstrong, H. A., Abbott, G. D., Turner, B. R., Makhlouf, I. M., Muhammad, A. B., Pedentchouk, N., et al. (2009). Black shale deposition in an Upper Ordovician–Silurian permanently stratified, peri-glacial basin, southern Jordan. *Palaeogeogr. Palaeoclimatol. Palaeoecol.* 273, 368–377. doi: 10.1016/j.palaeo.2008.05.005

Awan, R. S., Liu, C., Feng, D., Zang, Q., Wu, Y., and Ali, S. (2022). Origin of organic matter and depositional characteristics of early Cambrian Niutitang Formation from South China: New insights using molecular fossils. *Geol. J.* 58, 298–314. doi: 10.1002/gj.4593

Breit, G. N., and Wanty, R. B. (1991). Vanadium accumulation in carbonaceous rocks: A review of geochemical controls during deposition and diagenesis. *Chem. Geol.* 91, 83–97. doi: 10.1016/0009-2541(91)90083-4

Brumsack, H.-J. (2006). The trace metal content of recent organic carbon-rich sediments: Implications for Cretaceous black shale formation. *Palaeogeogr. Palaeoclimatol. Palaeoecol.* 232, 344–361. doi: 10.1016/j.palaeo.2005.05.011

Calvert, S. E., and Pedersen, T. F. (2007). Chapter Fourteen Elemental Proxies for Palaeoclimatic and Palaeoceanographic Variability in Marine Sediments: Interpretation and Application. *Develop. Mar. Geol.* 1, 567–644. doi: 10.1016/s1572-5480(07)01019-6

Chang, H., Chu, X., Feng, L., Huang, J., and Zhang, Q. (2009). Redox sensitive trace elements as paleoenvironments proxies. *GEOLOGIC. Rev.* 55, 91–99. doi: 10.16509/j.georeview.2009.01.014

Chen, X., Shi, W., Hu, Q., Hou, Y., Zhai, G., Dong, T., et al. (2022). Origin of authigenic quartz in organic-rich shales of the Niutitang Formation in the northern margin of Sichuan Basin, South China: Implications for pore network development. *Mar. Pet. Geol.* 138, 1–13. doi: 10.1016/j.marpetgeo.2022.105548

Choi, J. H., and Hariya, Y. (1992). Geochemistry and depositional environment of mn oxide deposits in the Tokoro belt, Northeastern Hokkaido, Japan. *Econ. Geol.* 87, 1265–1274. doi: 10.2113/gsecongeo.87.5.1265

Chou, C.-L. (2012). Sulfur in coals: A review of geochemistry and origins. *Int. J. Coal Geol.* 100, 1–13. doi: 10.1016/j.coal.2012.05.009

Condie, K. (1993). Chemical composition and evolution of the upper continental crust: Contrasting results from surface samples and shales. *Chem. Geol.* 104, 1–37. doi: 10.1016/0009-2541(93)90140-E

Cremonese, L., Shields-Zhou, G. A., Struck, U., Ling, H.-F., and Och, L. M. (2014). Nitrogen and organic carbon isotope stratigraphy of the Yangtze Platform during the

Ediacaran–Cambrian transition in South China. *Palaeogeogr. Palaeoclimatol. Palaeoecol.* 398, 165–186. doi: 10.1016/j.palaeo.2013.12.016

Crusius, J., Calvert, S., Pedersen, T., and Sage, D. (1996). Rhenium and molybdenum enrichments in sediments as indicators of oxic, suboxic and sulfidic conditions of deposition. *Earth Planet. Sci. Lett.* 145, 65–78. doi: 10.1016/S0012-821X(96)00204-X

Dai, S., Li, T., Seredin, V. V., Ward, C. R., Hower, J. C., Zhou, Y., et al. (2014). Origin of minerals and elements in the Late Permian coals, tonsteins, and host rocks of the Xinde Mine, Xuanwei, eastern Yunnan, China. *Int. J. Coal Geol.* 121, 53–78. doi: 10.1016/j.coal.2013.11.001

Dai, S., Seredin, V. V., Ward, C. R., Hower, J. C., Xing, Y., Zhang, W., et al. (2015). Enrichment of U–Se–Mo–Re–V in coals preserved within marine carbonate successions: geochemical and mineralogical data from the Late Permian Guiding Coalfield, Guizhou, China. *Miner. Deposita* 50, 159–186. doi: 10.1007/s00126-014-0528-1

Dai, S., Xie, P., Jia, S., Ward, C. R., Hower, J. C., Yan, X., et al. (2017). Enrichment of U-Re-V-Cr-Se and rare earth elements in the Late Permian coals of the Moxinpo Coalfield, Chongqing, China: Genetic implications from geochemical and mineralogical data. *Ore Geol. Rev.* 80, 1–17. doi: 10.1016/j.oregeorev.2016.06.015

Dai, S., Zhang, W., Seredin, V. V., Ward, C. R., Hower, J. C., Song, W., et al. (2013a). Factors controlling geochemical and mineralogical compositions of coals preserved within marine carbonate successions: A case study from the Heshan Coalfield, southern China. *Int. J. Coal Geol.* 109-110, 77–100. doi: 10.1016/j.coal.2013.02.003

Dai, S., Zhang, W., Ward, C. R., Seredin, V. V., Hower, J. C., Li, X., et al. (2013b). Mineralogical and geochemical anomalies of late Permian coals from the Fusui Coalfield, Guangxi Province, Southern China: Influences of terrigenous materials and hydrothermal fluids. *Int. J. Coal Geol.* 105, 60–84. doi: 10.1016/j.coal.2012.12.003

Dai, S., Zheng, X., Wang, X., Finkelman, R. B., Jiang, Y., Ren, D., et al. (2018). Stone coal in China: a review. *Int. Geol. Rev.* 60, 736–753. doi: 10.1080/00206814.2017.1378131

DeBaar, H. J. W., Bacon, M. P., and Brewer, P. G. (1985). Rare earth elements in the Pacific and Atlantic Oceans. *Genchimica Cosmochimica Acta* 49, 1946–1959. doi: 10.1016/0016-7037(85)90089-4

Dehairs, F., Lambert, C. E., Chesselet, R., and Risler, N. (1987). The biological production of marine suspended barite and the barium cycle in the Western Mediterranean Sea. *Biogeochemistry* 4, 119–139. doi: 10.1007/BF02180151

Delabroye, A., and Vecoli, M. (2010). The end-Ordovician glaciation and the Hirnantian Stage: A global review and questions about Late Ordovician event stratigraphy. *Earth Sci. Rev.* 98, 269–282. doi: 10.1016/j.earscirev.2009.10.010

Ding, Y., Li, Z., Liu, S., Song, J., Zhou, X., Sun, W., et al. (2021). Sequence stratigraphy and tectono-depositional evolution of a late Ediacaran epeiric platform in the upper Yangtze area, South China. *Precambrian Res.* 354, 1–24. doi: 10.1016/j.precamres.2020.106077

Dong, T., He, Q., He, S., Zhai, G., Zhang, Y., Wei, S., et al. (2021). Quartz types, origins and organic matter-hosted pore systems in the lower cambrian Niutitang Formation, middle yangtze platform, China. *Mar. Pet. Geol.* 123, 1–21. doi: 10.1016/j.marpetgeo.2020.104739

Dymond, J., Suess, E., and Lyle, M. (1992). Barium in deep-sea sediment: a geochemical proxy for paleoproductivity. *PALEOCEANOGRAPHY* 7, 163–181. doi: 10.1029/92PA00181

Eagle, M., Paytan, A., Arrigo, K. R., van Dijken, G., and Murray, R. W. (2003). A comparison between excess barium and barite as indicators of carbon export. *Paleoceanography* 18, 1–21. doi: 10.1029/2002PA000793

Fathy, D., Baniasad, A., Littke, R., and Sami, M. (2024). Tracing the geochemical imprints of Maastrichtian black shales in southern Tethys, Egypt: Assessing hydrocarbon source potential and environmental signatures. *Int. J. Coal Geol.* 283, 1–17. doi: 10.1016/j.coal.2024.104457

Fu, W., Hu, W., Cai, Q., Wei, S., She, J., Wang, X., et al. (2023a). Sedimentary environment and organic accumulation of the Ordovician–Silurian black shale in Weiyuan, Sichuan Basin, China. *Minerals* 13, 1–19. doi: 10.3390/min13091161

Fu, X., Xu, L., Yan, H., Ye, H., and Ding, J. (2023b). Mineralogy and trace element geochemistry of the early Cambrian black shale-hosted Zhongcun vanadium deposit, southern Qinling, China. *Ore Geol. Rev.* 155, 1–22. doi: 10.1016/j.oregeorev.2023.105371

Fu, Y., Dong, L., Li, C., Qu, W., Pei, H., Qiao, W., et al. (2016). New Re-Os isotopic constrains on the formation of the metalliferous deposits of the Lower Cambrian Niutitang formation. *J. Earth Sci.* 27, 271–281. doi: 10.1007/s12583-016-0606-7

Gao, B., Liu, Z., Shu, Z., Liu, H., Wang, R., Jin, Z., et al. (2020). Reservoir characteristics and exploration of the Lower Cambrian shale gas in the Middle-Upper Yangtze area. *Oil & Gas Geol.* 41, 284–294. doi: 10.11743/ogg20200205

Gao, J., Zhang, J.-k., He, S., Zhao, J.-x., He, Z.-l., Wo, Y.-j., et al. (2019). Overpressure generation and evolution in Lower Paleozoic gas shales of the Jiaoshiba region, China: Implications for shale gas accumulation. *Mar. Pet. Geol.* 102, 844–859. doi: 10.1016/j.marpetgeo.2019.01.032

Gao, P., Xiao, X., Meng, G., Lash, G. G., Li, S., and Han, Y. (2023). Quartz types and origins of the Upper Permian Dalong Formation shale of the Sichuan Basin: Implications for pore preservation in deep shale reservoirs. *Mar. Pet. Geol.* 156, 1–14. doi: 10.1016/j.marpetgeo.2023.106461

Ghosh, S., and Sarkar, S. (2010). Geochemistry of Permo-Triassic mudstone of the Satpura Gondwana basin, central India: Clues for provenance. *Chem. Geol.* 277, 78–100. doi: 10.1016/j.chemgeo.2010.07.012

Gonneea, M. E., and Paytan, A. (2006). Phase associations of barium in marine sediments. *Mar. Chem.* 100, 124–135. doi: 10.1016/j.marchem.2005.12.003

Han, S., Zhang, J., Wang, C., Tang, X., and Chen, Z. Q. (2018). Elemental geochemistry of lower Silurian Longmaxi shale in southeast Sichuan Basin, South China: Constraints for Paleoenvironment. *Geol. J.* 53, 1458–1464. doi: 10.1002/gj.2966

Han, T., Zhu, X., Li, K., Jiang, L., Zhao, C., and Wang, Z. (2015). Metal sources for the polymetallic Ni–Mo–PGE mineralization in the black shales of the Lower Cambrian Niutitang Formation, South China. *Ore Geol. Rev.* 67, 158–169. doi: 10.1016/j.oregeorev.2014.11.020

Hayashi, K.-I., Fujisawa, H., Holland, H. D., and Ohmoto, H. (1997). Geochemistry of ~ 1.9 Ga sedimentary rocks from northeastern Labrador, Canada. *Geochim. Cosmochim. Acta* 61, 4115–4137. doi: 10.1016/S0016-7037(97)00214-7

Hu, J. (2019). Study on geological conditions of shale gas accumulation in the lower Cambrian Shuijing formation of the Huangling domal in western Hubei province. *ChengDu Univ. Technol.* 2020, 1–83. doi: 10.26986/d.cnki.gcdlc.2019.000622

Huang, B., Tian, H., Wilkins, R. W. T., Xiao, X., and Li, L. (2013). Geochemical characteristics, palaeoenvironment and formation model of Eocene organic-rich shales in the Beibuwan Basin, South China Sea. *Mar. Pet. Geol.* 48, 77–89. doi: 10.1016/j.marpetgeo.2013.07.012

Jia, Z. (2018). Geochemistry characteristics of hydrothermal sedimentation in the Lower Cambrian Niutitang Formation in Guizhou. *China Univ. Geosci.* 2022, 1–130. doi: 10.27493/d.cnki.gzdzy.2018.000161

Jones, B., and Manning, D. A. C. (1994). Comparison of geochemical indices used for the interpretation of palaeoredox conditions in ancient mudstones. *Chem. Geol.* 111, 111–129. doi: 10.1016/0009-2541(94)90085-X

Kidder, D. L., and Erwin, D. H. (2001). Secular distribution of biogenic silica through the phanerozoic: comparison of silica-replaced fossils and bedded cherts at the series level. *J. Geology* 109, 509–522. doi: 10.1086/320794

Lézin, C., Andreu, B., Pellenard, P., Bouchez, J.-L., Emmanuel, L., Fauré, P., et al. (2013). Geochemical disturbance and paleoenvironmental changes during the Early Toarcian in NW Europe. *Chem. Geol.* 341, 1–15. doi: 10.1016/j.chemgeo.2013.01.003

Li, T., Gao, H., Wang, C., Cheng, Z., Yang, Y., and Zhan, J. (2022). The accumulation model of organic matters for the Niutitang Formation shale and its control on the pore structure: a case study from Northern Guizhou. *J. Pet. Explor. Prod. Technol.* 12, 2047–2065. doi: 10.1007/s13202-021-01452-3

Li, D., Li, R., Zhu, Z., Wu, X., Cheng, J., Liu, F., et al. (2017a). Origin of organic matter and paleo-sedimentary environment reconstruction of the Triassic oil shale in Tongchuan City, Southern Ordos Basin (China). *Fuel* 208, 223–235. doi: 10.1016/j.fuel.2017.07.008

Li, D., Li, R., Zhu, Z., Wu, X., Liu, F., Zhao, B., et al. (2017b). Elemental characteristics and paleoenvironment reconstruction: a case study of the Triassic lacustrine Zhangjiatan oil shale, southern Ordos Basin, China. *Acta Geochim.* 37, 134–150. doi: 10.1007/s11631-017-0193-z

Li, D., Li, R., Zhu, Z., and Xu, F. (2017c). Elemental characteristics of lacustrine oil shale and its controlling factors of palaeo-sedimentary environment on oil yield: a case from Chang 7 oil layer of Triassic Yanchang Formation in southern Ordos Basin. *Acta Geochim.* 37, 228–243. doi: 10.1007/s11631-017-0206-y

Liu, Q. (2017). Element geochemical characteristics of source rocks in the Shahejie Formation in Well Fangye-1, Dongying sag and their geological significance. *Petrol. Geol. Recovery Efficiency* 24, 40–52. doi: 10.13673/j.cnki.cn37-1359/te.2017.05.006

Liu, Z., Yan, D., and Niu, X. (2020). Insights into pore structure and fractal characteristics of the lower Cambrian niutitang formation shale on the Yangtze platform, South China. *J. Earth Sci.* 31, 169–180. doi: 10.1007/s12583-020-1259-0

Luning, S., Craig, J., Loydell, D. K., Storch, P., and Fitches, B. (2000). Lower Silurian 'hot shales' in North Africa and Arabia: regional distribution and depositional model. *Earth-Sci. Rev.* 49, 121–200. doi: 10.1016/S0012-8252(99)00060-4

Luo, Q., Zhong, N., Zhu, L., Wang, Y., Qin, J., Qi, L., et al. (2013). Correlation of burial organic carbon and paleoproductivity in the mesoproterozoic hongshuizhuang formation, northern north china. *Chin. Sci. Bull.* 58, 1299–1309. doi: 10.1007/s11434-012-5534-z

McLennan, S. M. (2001a). Relationships between the trace element composition of sedimentary rocks and upper continental crust. *Geochem. Geophys. Geosyst.* 2. doi: 10.1029/2000GC000109

McLennan, S. M. (2001b). Relationships between the trace element composition of sedimentary rocks and upper continental crust. *Geochem. Geophys. Geosyst.* 2. doi: 10.1029/2000GC000109

Mohammed, I. Q., Farouk, S., Baioumy, H., Lotfy, N. M., and Al-Hadidy, A. H. (2020). Mineralogical and geochemical characteristics of the Paleozoic source rocks, Akkas gas field, Western Desert of Iraq: Implications for their origin, maturation and Ordovician-Silurian transition. *Mar. Pet. Geol.* 118, 1–18. doi: 10.1016/j.marpetgeo.2020.104432

Morforda, J. L., Russell, A. D., and Emerson, S. (2001). Trace metal evidence for changes in the redox environment associated with the transition from terrigenous clay to diatomaceous sediment, Saanich Inlet, BC. *Mar. Geol.* 174, 355–369. doi: 10.1016/S0025-3227(00)00160-2

Murphy, A. E., Sageman, B. B., Hollander, D. J., Lyons, T. W., and Brett, C. E. (2000). Black shale deposition and faunal overturn in the Devonian Appalachian Basin: Clastic starvation, seasonal water-column mixing, and efficient biolimiting nutrient recycling. *Paleoceanography* 15, 280–291. doi: 10.1029/1999PA000445

Murray, R. W. (1994). Chemical criteria to identify the depositional environment of chert: general principles and applications. *Sediment. Geol.* 90, 213–232. doi: 10.1016/0037-0738(94)90039-6

Murray, R. W., and Leinen, M. (1993). Biogenic flux of al to sediment in the central equatorial pacific ocean: evidence for increased productivity during glacial periods. *PALEOCEANOGRAPHY* 8, 651–670. doi: 10.1029/93PA02195

Murray, R. W., and Leinen, M. (1996). Scavenged excess aluminum and its relationship to bulk titanium in biogenic sediment from the central equatorial pacific ocean. *Geochim. Cosmochim. Acta* 60, 3869–3878. doi: 10.1016/0016-7037(96)00236-0

Mustafa, K. A., Sephton, M. A., Watson, J. S., Spathopoulos, F., and Krzywiec, P. (2015). Organic geochemical characteristics of black shales across the Ordovician–Silurian boundary in the Holy Cross Mountains, central Poland. *Mar. Pet. Geol.* 66, 1042–1055. doi: 10.1016/j.marpetgeo.2015.08.018

Och, L. M., Shields-Zhou, G. A., Poulton, S. W., Manning, C., Thirlwall, M. F., Li, D., et al. (2013). Redox changes in Early Cambrian black shales at Xiaotan section, Yunnan Province, South China. *Precambrian Res.* 225, 166–189. doi: 10.1016/j.precamres.2011.10.005

Paytan, A., Kastner, M., and Chavez, F. P. (1996). Glacial to interglacial fluctuations in productivity in the equatorial pacific as indicated by marine barite. *Science* 274, 1355–1357. doi: 10.1126/science.274.5291.1355

Piper, D. Z., and Perkins, R. B. (2004). A modern vs. Permian black shale—the hydrography, primary productivity, and water-column chemistry of deposition. *Chem. Geol.* 206, 177–197. doi: 10.1016/j.chemgeo.2003.12.006

Pohl, A., Donnadieu, Y., Le Hir, G., and Ferreira, D. (2017). The climatic significance of Late Ordovician-early Silurian black shales. *Paleoceanography* 32, 397–423. doi: 10.1002/2016PA003064

Rachold, V., and Brumsack, H.-J. (2001). Inorganic geochemistry of Albian sediments from the Lower Saxony Basin NW Germany: palaeoenvironmental constraints and orbital cycles. *Palaeogeogr. Palaeoclimatol. Palaeoecol.* 174, 121–143. doi: 10.1016/S0031-0182(01)00290-5

Rimmer, S. M. (2004). Geochemical paleoredox indicators in Devonian–Mississippian black shales, Central Appalachian Basin (USA). *Chem. Geol.* 206, 373–391. doi: 10.1016/j.chemgeo.2003.12.029

Rimmer, S. M., Thompson, J. A., Goodnight, S. A., and Robl, T. L. (2004). Multiple controls on the preservation of organic matter in Devonian–Mississippian marine black shales: geochemical and petrographic evidence. *Palaeogeogr. Palaeoclimatol. Palaeoecol.* 215, 125–154. doi: 10.1016/S0031-0182(04)00466-3

Roser, B., and Korsch, R. (1986). Determination of tectonic setting of sandstone-mudstone suites using SiO2 content and K2O/Na2O ratio. *J. Geol.* 94, 635–650. doi: 10.1086/629071

Sadiq, M. (1988). Thermodynamic solubility relationships of inorganic vanadium in the marine environment. *Mar. Chem.* 23, 87–96. doi: 10.1016/0304-4203(88)90024-2

Schoepfer, S. D., Shen, J., Wei, H., Tyson, R. V., Ingall, E., and Algeo, T. J. (2015). Total organic carbon, organic phosphorus, and biogenic barium fluxes as proxies for paleomarine productivity. *Earth Sci. Rev.* 149, 23–52. doi: 10.1016/j.earscirev.2014.08.017

Shao, L., Zhang, P., Ren, D., and Lei, J. (1998). Late Permian coal-bearing carbonate successions in southern China: coal accumulation on carbonate platforms. *Int. J. Coal Geol.* 37, 235–256. doi: 10.1016/S0166-5162(98)00008-1

Sheets, H. D., Mitchell, C. E., Melchin, M. J., Loxton, J., Storch, P., Carlucci, K. L., et al. (2016). Graptolite community responses to global climate change and the Late Ordovician mass extinction. *Proc. Natl. Acad. Sci. U.S.A.* 113, 8380–8385. doi: 10.1073/pnas.1602102113

Smolarek, J., Marynowski, L., Trela, W., Kujawski, P., and Simoneit, B. R. T. (2017). Redox conditions and marine microbial community changes during the end-Ordovician mass extinction event. *Global Planet. Change* 149, 105–122. doi: 10.1016/j.gloplacha.2017.01.002

Sugisaki, R., Ido, M., Takeda, H., Isobe, Y., Hayashi, Y., Nakamura, N., et al. (1983). Origin of hydrogen and carbon dioxide in fault gases and its relation to fault activity. *J. Geology* 91, 239–258. doi: 10.1086/628769

Taylor, S. R., and McLennan, S. M. (1995). The geochemical evolution of the continental crust. *Rev. Geophys.* 33, 241–265. doi: 10.1029/95RG00262

Taylor, S. R., and McLennan, S. M. (1985). *The continental crust: Its composition and evolution* (Blackwell, Oxford). Available at: https://www.osti.gov/biblio/6582885.

Tian, T., Zhou, S., Fu, D., Yang, F., and Li, J. (2019). Characterization and controlling factors of pores in the Lower Cambrian Niutitang shale of the Micangshan Tectonic Zone, SW China. *Arabian J. Geosci.* 12, 1–14. doi: 10.1007/s12517-019-4407-z

Trela, W., Podhalańska, T., Smolarek, J., and Marynowski, L. (2016). Llandovery green/grey and black mudrock facies of the northern Holy Cross Mountains (Poland) and their relation to early Silurian sea-level changes and benthic oxygen level. *Sediment. Geol.* 342, 66–77. doi: 10.1016/j.sedgeo.2016.06.003

Tribovillard, N., Algeo, T. J., Baudin, F., and Riboulleau, A. (2012). Analysis of marine environmental conditions based onmolybdenum–uranium covariation—Applications to Mesozoic paleoceanography. *Chem. Geol.* 324-325, 46–58. doi: 10.1016/j.chemgeo.2011.09.009

Tribovillard, N., Algeo, T. J., Lyons, T., and Riboulleau, A. (2006). Trace metals as paleoredox and paleoproductivity proxies: An update. *Chem. Geol.* 232, 12–32. doi: 10.1016/j.chemgeo.2006.02.012

Tribovillard, N., Averbuch, O., Devleeschouwer, X., Racki, G., and Riboulleau, A. (2004). Deep-water anoxia over the Frasnian–Famennian boundary (La Serre, France): a tectonically induced oceanic anoxic event? *Terra Nova* 16, 288–295. doi: 10.1111/j.1365-3121.2004.00562.x

Vinogradov, V. (1986). Strontium isotopic composition and problems of genesis of anorthosites. *Izvestiya akademii nauk sssr seriya geologicheskaya*. 8–15.

Vosoughi Moradi, A., Sarı, A., and Akkaya, P. (2016). Geochemistry of the Miocene oil shale (Hançili Formation) in the Çankırı-Çorum Basin, Central Turkey: Implications for Paleoclimate conditions, source–area weathering, provenance and tectonic setting. *Sediment. Geol.* 341, 289–303. doi: 10.1016/j.sedgeo.2016.05.002

Wan, Y., Zhang, S., Tang, S., Pan, Z., and Wu, W. (2018). A comparative study of characterization of lower Palaeozoic Niutitang shale in northwestern Hunan, China. *J. Nat. Gas Sci. Eng.* 53, 284–300. doi: 10.1016/j.jngse.2018.03.015

Wang, Z., Tan, J., Hilton, J., Dick, J., and Wen, Z. (2023). Trace element enrichment mechanisms in black shales during the early cambrian (ca. 521–514 Ma), South China. *Mar. Pet. Geol.* 149, 1–13. doi: 10.1016/j.marpetgeo.2022.106083

Wedepohl, K. (1991). Chemical composition and fractionation of the continental crust. *Geol. Rundsch.* 80, 207–223. doi: 10.1007/BF01829361

Wei, H., Feng, Q., Yu, J., and Chang, S. (2022). Characteristics and sources of organic matter from the early Cambrian niutitang formtion and its preservation environment in Guizhou. *J. Earth Sci.* 33, 933–944. doi: 10.1007/s12583-020-1371-1

Wignall, P. B. (1994). 1.Sequence stratigraphy - applications to basins in Northern England: Leeds, UK. *J. Pet. Geol.* 17, 243–243. doi: 10.1111/j.1747-5457.1994.tb00129.x

Wignall, P. B., and Myers, K. J. (1998). Interpreting benthic oxygen levels in mudrocks: A new approach. *GEOLOGY* 16, 452–455. doi: 10.1130/0091-7613(1988)016<0452:IBOLIM>2.3.CO;2

Wójcik-Tabol, P., and Ślączka, A. (2009). "Provenance and diagenesis of siliciclastic and organic material in the albian-turonian sediments (Silesian nappe, lanckorona, outer carpathians, poland): preliminary studies," in *Annales societatis geologorum poloniae: Polskie towarzystwo geologiczne*, 53–66.

Wright, J., Schrader, H., and holser, W. T. (1987). Paleoredox variations in ancient oceans recorded by rare earth elements in fossil apatite. *Geochim. Cosmochim. Acta* 51, 631–644. doi: 10.1016/0016-7037(87)90075-5

Wu, C., Zhang, L., Zhang, T., Tuo, J., Song, D., Liu, Y., et al. (2020). Reconstruction of paleoceanic redox conditions of the lower Cambrian Niutitang shales in northern Guizhou, Upper Yangtze region. *Palaeogeogr. Palaeoclimatol. Palaeoecol.* 538, 1–11. doi: 10.1016/j.palaeo.2019.109457

Wu, K., Zhang, T., Yang, Y., Sun, Y., and Yuan, D. (2016). Contribution of oxygenic photosynthesis to palaeo-oceanic organic carbon sink fluxes in Early Cambrian Upper Yangtze shallow sea: Evidence from black shale record. *J. Earth Sci.* 27, 211–224. doi: 10.1007/s12583-016-0693-5

Wu, Y., Fan, T., Jiang, S., Yang, X., Ding, H., Meng, M., et al. (2015). Methane adsorption capacities of the lower paleozoic marine shales in the Yangtze platform, South China. *Energy Fuels* 29, 4160–4167. doi: 10.1021/acs.energyfuels.5b00286

Xi, Z., Tang, S., and Wang, J. (2018). The reservoir characterization and shale gas potential of the Niutitang formation: Case study of the SY well in northwest Hunan Province, South China. *J. Petrol. Sci. Eng.* 171, 687–703. doi: 10.1016/j.petrol.2018.08.002

Xia, P., Hao, F., Tian, J., Zhou, W., Fu, Y., Guo, C., et al. (2022). Depositional environment and organic matter enrichment of early Cambrian niutitang black shales in the upper Yangtze Region, China. *Energies* 15, 1–21. doi: 10.3390/en15134551

Xu, L., Lehmann, B., and Mao, J. (2013). Seawater contribution to polymetallic Ni–Mo–PGE–Au mineralization in Early Cambrian black shales of South China: Evidence from Mo isotope, PGE, trace element, and REE geochemistry. *Ore Geol. Rev.* 52, 66–84. doi: 10.1016/j.oregeorev.2012.06.003

Yan, D., Chen, D., Wang, Q., and Wang, J. (2010). Large-scale climatic fluctuations in the latest Ordovician on the Yangtze block, south China. *Geology* 38, 599–602. doi: 10.1130/G30961.1

Yan, D., Li, S., Fu, H., Jasper, D. M., Zhou, S., Yang, X., et al. (2021). Mineralogy and geochemistry of Lower Silurian black shales from the Yangtze platform, South China. *Int. J. Coal Geol.* 237, 1–18. doi: 10.1016/j.coal.2021.103706

Yan, D., Wang, H., Fu, Q., Chen, Z., He, J., and Gao, Z. (2015). Geochemical characteristics in the Longmaxi Formation (Early Silurian) of South China: Implications for organic matter accumulation. *Mar. Pet. Geol.* 65, 290–301. doi: 10.1016/j.marpetgeo.2015.04.016

Yang, J., and Yi, F. (2012). A study on occurrence modes and enrichment patterns of lower Cambrian black shale series in northern Guizhou province, China. *Acta Mineral. Sin.* 32, 281–287. doi: 10.16461/j.cnki.1000-4734.2012.02.022

Yang, X. (2020). Depositional environment and organic matter accumulation of the Lower Cambrian Niutitang Formation shale in northern Guizhou. *China Univ. Geosciences.* 2020, 1–77. doi: 10.27493/d.cnki.gzdzy.2020.000329

Yang, X., Zhu, M., Zhao, Y., Zhang, J., Guo, Q., and Pi, D. (2008). REE geoche mical characteristics of the Ediacaran-Lower cambrian black rock series i n eastern guizhou. *Geological Rev.* 54, 3–15. doi: 10.16509/j.georeview.2008.01.003

Ye, J., and Fan, D. (2000). Characteristics and mineralization of ore deposits related to black shale series. *Bull. Mineral. Petrol. Geochem.* 19, 95–102.

Ye, Y., Tang, S., Xi, Z., Jiang, D., and Duan, Y. (2022). Quartz types in the Wufeng-Longmaxi Formations in southern China: Implications for porosity evolution and shale brittleness. *Mar. Pet. Geol.* 137, 1–15. doi: 10.1016/j.marpetgeo.2021.105479

Yi, X., Ji, X., Huang, Y., Liu, Z., and Meng, J. (2022). Black shale paleo-environmental reconstructions: A geochemical case study of two Ordovician–Silurian boundary sections in middle Yangtze area, China. *Front. Earth Sci.* 10. doi: 10.3389/feart.2022.842752

Yin, L.-M., Borjigin, T., Knoll, A. H., Bian, L.-Z., Xie, X.-M., Bao, F., et al. (2017). Sheet-like microfossils from hydrothermally influenced basinal cherts of the lower Cambrian (Terreneuvian) Niutitang Formation, Guizhou, South China. *Palaeoworld* 26, 1–11. doi: 10.1016/j.palwor.2016.01.005

Zhai, L., Wu, C., Ye, Y., Zhang, S., and Wang, Y. (2018). Fluctuations in chemical weathering on the Yangtze Block during the Ediacaran–Cambrian transition: Implications for paleoclimatic conditions and the marine carbon cycle. *Palaeogeogr. Palaeoclimatol. Palaeoecol.* 490, 280–292. doi: 10.1016/j.palaeo.2017.11.006

Zhang, H., Wu, J., Jin, X., and Li, G. (2018). The genetic type and its geological indication significance of shale minerals in Niutitang Formation. *Coal Geol. Explor.* 46, 61–67. doi: 10.3969/j.issn.1001-1986.2018.02.010

Zhang, J., Xu, H., Zhou, Z., Ren, P., Guo, J., and Wang, Q. (2019). Geological characteristics of shale gas reservoir in Yichang area, western Hubei. *Acta Petrolei Sin.* 40, 887–899. doi: 10.7623/syxb201908001

Zhang, K., Li, X., Wang, Y., Liu, W., Yu, Y., Zhou, L., et al. (2021). Paleo-environments and organic matter enrichment in the shales of the Cambrian Niutitang and Wunitang Formations, south China: Constraints from depositional environments and geochemistry. *Mar. Pet. Geol.* 134, 1–11. doi: 10.1016/j.marpetgeo.2021.105329

Zhang, K., Liu, R., Bai, E., Zhao, Z., Peyrotty, G., Fathy, D., et al. (2023). Biome responses to a hydroclimatic crisis in an Early Cretaceous (Barremian–Aptian) subtropical inland lake ecosystem, Northwest China. *Palaeogeogr. Palaeoclimatol. Palaeoecol.* 622, 1–22. doi: 10.1016/j.palaeo.2023.111596

Zhang, Q., Wang, J., Yu, Q., Wang, X., Zhao, A., and Lei, Z. (2017). Geochemical features and paleoenvironment of shales in longmaxi formation of complicated structure area, Southwestern Sichuan basin. *Xinjiang Petrol. Geol.* 38, 399–406. doi: 10.7657/XJPG20170404

Zhang, Z.-F., Zhang, Z.-L., Li, G.-X., and Holmer, L. E. (2016). The Cambrian brachiopod fauna from the first-trilobite age Shuijingtuo Formation in the Three Gorges area of China. *Palaeoworld* 25, 333–355. doi: 10.1016/j.palwor.2015.10.001

Zhao, J., Jin, Z., Lin, C., Liu, G., Liu, K., Liu, Z., et al. (2019). Sedimentary environment of the Lower Cambrian Qiongzhusi Formation shale in the Upper Yangtze region. *Oil & Gas Geol.* 40, 7.1–715. doi: 10.11743/ogg20190402

Zhao, L., Dai, S., Graham, I. T., Li, X., and Zhang, B. (2016). New insights into the lowest Xuanwei Formation in eastern Yunnan Province, SW China: Implications for Emeishan large igneous province felsic tuff deposition and the cause of the end-Guadalupian mass extinction. *Lithos* 264, 375–391. doi: 10.1016/j.lithos.2016.08.037

Zhou, X., Liu, Y., Cao, H., Zhong, H., and Li, Y. (2021). Responses of oceanic chemistry to climatic perturbations during the Ordovician-Silurian transition: Implications for geochemical proxies and organic accumulations. *Mar. Pet. Geol.* 134, 1–13. doi: 10.1016/j.marpetgeo.2021.105341

Zhou, H. (2019). Geochemical characteristics and geological significance of the lower cambrian black rock series in northwestern hunan. *East China Univ. Technol.* 2020, 1–61.

Zhu, G., Wang, T., Xie, Z., Xie, B., and Liu, K. (2015). Giant gas discovery in the Precambrian deeply buried reservoirs in the Sichuan Basin, China: Implications for gas exploration in old cratonic basins. *Precambrian Res.* 262, 45–66. doi: 10.1016/j.precamres.2015.02.023

Zhu, G., Zhao, K., Li, T., Zhang, Z., Tang, S., and Wang, P. (2021). Anomalously high enrichment of mercury in early Cambrian black shales in South China. *J. Asian Earth Sci.* 216, 1–13. doi: 10.1016/j.jseaes.2021.104794